Computerization, Persistent Returns, and Wealth Concentration

Musa Orak*

October 2026

Abstract

Computerization has opposing long-run effects on wealth concentration through changes in wages and capital accumulation and through widening persistent return differences. I combine an estimated task-based technology with incomplete markets and endogenous schooling, and compare stationary equilibria using U.S. inputs from 1967 to 2019. The ICT-linked return rule allows the dispersion of persistent household returns to rise with computer capital. I calibrate its elasticity, ψ, to the observed 7.2-point rise in the top-1% wealth share. With this rule active ($\psi = \psi^{\star}$), the induced widening more than offsets the equalizing response at fixed premia: the ICT-price decline raises the stationary top-1% wealth share by 6.5 percentage points, holding depreciation and education costs at their 2019 values. Holding return premia at either their initial or baseline 2019 distribution, the same price decline instead lowers the share by 8.1–8.6 percentage points. Higher wages and adjustments in the common return and financing tax both contribute to this decline, even as employment polarizes. At the 2019 benchmark inputs, wider dispersion raises the top-1% wealth share by about 14 percentage points relative to the economy retaining its initial dispersion ($\psi = 0$). This contribution depends strongly on persistence: shortening return-type spells from 4.6 to 2.1 years reduces it by about two-thirds. Sustained return advantages concentrate wealth while inducing capital accumulation that lowers the common return.

JEL: D31, E21, J24, O33, E25.

Keywords: job polarization; wealth concentration; inequality; computerization; heterogeneous returns; incomplete markets.

*Division of International Finance, Board of Governors of the Federal Reserve System, Washington, D.C. 20551, United States. E-mail: musa.orak@frb.gov. An earlier version appeared as Chapter 3 of the author's doctoral dissertation (Orak, 2016) under the title "Job Polarization, Skill Accumulation and Wealth Inequality." The views in this paper are solely the responsibility of the author and should not be interpreted as reflecting the views of the Board of Governors of the Federal Reserve System or of any other person associated with the Federal Reserve System.

1 Introduction

Between 1967 and 2019, the price of computing equipment in the United States fell by a factor of nearly four hundred. Over the same period, employment shifted out of routine occupations toward abstract and manual ones (Autor, Levy, and Murnane, 2003; Autor and Dorn, 2013; Goos, Manning, and Salomons, 2014; Cortes, Jaimovich, and Siu, 2017), college attainment nearly tripled, and the top-1% wealth share rose by about 7 percentage points (Saez and Zucman, 2016; Smith, Zidar, and Zwick, 2023; World Inequality Database, 2022). A leading explanation for these labor-market changes is computerization: computers substitute for routine tasks and complement abstract ones, raising abstract wages relative to routine wages and increasing the payoff to schooling. Whether the same force concentrated wealth is less clear. Higher wages for a growing group of abstract workers and rising college attainment could spread wealth more broadly. The rise of artificial intelligence gives this question renewed importance: its effects on wage inequality and wealth concentration need not have the same sign (Rockall, Mendes Tavares, and Pizzinelli, 2025). The computerization episode provides a benchmark for examining how labor-market adjustment and persistent differences in household returns shape the distribution of wealth.

This paper quantifies two opposing long-run wealth effects of computerization. Cheaper computers change wages, schooling, and capital accumulation in ways that reduce top wealth concentration at fixed return premia. In the calibrated model, allowing persistent return differences to widen with computer capital more than offsets this decline and produces rising top wealth concentration.

I build a general-equilibrium model with three ingredients. Production uses structural capital, computer capital, and abstract, routine, and manual labor in a nested-CES technology in the tradition of Krusell et al. (2000), estimated by GMM on 1967–2019 U.S. data.[1] Households face uninsurable income risk, choose at birth whether to attend college, and sort across tasks by comparative advantage. They also earn persistently different returns on wealth, consistent with administrative evidence (Fagereng et al., 2020; Bach, Calvet, and Sodini, 2020). I feed the model the measured decline in computer-capital prices, together with benchmark-specific ICT depreciation and education

[1] Throughout the paper, "computer capital" refers to information and communications technology (ICT) capital, while "structural capital" refers to non-ICT capital. I use each pair of terms interchangeably.

costs, and compare stationary equilibria at the 1967, 1979, 1999, and 2019 benchmarks.[2]

The return channel links the dispersion of persistent household returns to the stock of computer capital, with elasticity ψ. I refer to this relationship as the ICT-linked return rule. With the channel inactive ($\psi = 0$), households retain persistent return differences at their 1967 dispersion. With the channel active ($\psi = \psi^\star$), dispersion widens as computer capital accumulates. The economic motivation is that computerization can increase the scale advantages of leading firms and the investment advantages of sophisticated households (Bessen, 2020; Lashkari, Bauer, and Boussard, 2024; Kacperczyk, Nosal, and Stevens, 2019). I calibrate $\psi^\star$ to the observed 1967–2019 increase in the top-1% wealth share, measuring the strength of the assumed link required to match that increase. Return persistence is calibrated to the initial top-1% share, while initial return dispersion is anchored to administrative evidence. The counterfactuals separate the ICT-price effect at fixed premia from the additional effect of widening persistent return differences.

With the return channel active ($\psi = \psi^\star$), lowering the ICT price from its 1967 to its 2019 value raises the top-1% wealth share by 6.50 percentage points, holding depreciation and education costs at their 2019 values. Cheaper ICT expands computer capital and, through the calibrated ICT-linked rule, widens persistent return differences. This concentrating force more than offsets the equalizing response through wages and common-return and tax adjustments. Holding the ICT price and all other inputs at their 2019 values, wider dispersion raises the top-1% share by 13.98 percentage points relative to the economy retaining its initial dispersion ($\psi = 0$).

The equalizing response becomes clear when return premia are held fixed as the ICT price falls. Under either the initial premium distribution or the wider baseline 2019 distribution, the same price decline lowers the top-1% wealth share by 8.14–8.61 percentage points. In both comparisons, employment shifts from routine work toward abstract and manual tasks, college attainment rises, and the common return falls. Wages rise in all three tasks, and median wealth increases. Cheaper ICT therefore generates employment polarization while spreading wealth more broadly when persistent return differences remain fixed.

A partial-equilibrium decomposition separates the decline under fixed premia into changes in task wages and changes in the common return together with the lump-sum financing tax.

[2]The sample ends in 2019 to study the long-run computerization episode separately from the labor-market disruptions associated with the COVID-19 pandemic.

Households adjust saving, occupation, and schooling at the specified prices and tax. Both adjustments reduce top wealth concentration. Averaging their contributions across the two possible orders, the common return and tax account for about three-quarters of the decline at initial premia. At wider 2019 premia, higher task wages account for more than half.

The production structure matters for the level of wealth concentration as well as for employment. Replacing the estimated technology with a tangent Cobb–Douglas technology raises the 2019 top-1% share by about 4.1–4.3 points at the two premium distributions, while substantially reducing the college expansion. Yet the effect of widening return dispersion remains almost unchanged. Across this comparison and the experiments with financing, ICT depreciation, and education costs, wider dispersion adds 12.9–14.2 points to the 2019 share. Restricting college entry changes this contribution by at most half a point. Wider dispersion also lowers college attainment by about three points in 2019, because a more concentrated wealth distribution leaves more newborns below the tuition threshold.

The duration of return advantages is central to their effect on wealth concentration. At fixed cross-sectional dispersion, shortening expected return-type spells from 4.6 to 2.1 years reduces the contribution of widening dispersion by about two-thirds. Sustained advantages allow high-return households to compound their wealth. Their additional saving expands the capital stock and lowers the common return even as wealth concentrates. The shape and scale of the return distribution and the upper asset bound also affect quantitative magnitudes. The ICT-price effects retain their signs under the alternative persistence calibration and at a wider asset bound.

Related literature. The closest related papers are Moll, Rachel, and Restrepo (2022), Koru (2024), and Prettner and Strulik (2020), which study the wealth-distribution effects of automation. Moll, Rachel, and Restrepo (2022) show that automation can increase wealth inequality by raising returns to capital relative to wages. Here, concentration rises through widening persistent differences in household returns, *even as the common return falls.* This paper takes up their call for quantitative work on the interaction between technology and persistent return heterogeneity. Koru (2024) endogenizes return dispersion through collateral-constrained entrepreneurship. Muto, Nakamura, and Nirei (2024) study digitalization in a model where risk-tolerant households hold most risky digital capital and earn higher returns as digitalization advances. I combine a reduced-form return process with

an estimated three-task technology and endogenous schooling to quantify how persistent return advantages interact with labor-market adjustment. Prettner and Strulik (2020) combine automation and endogenous education in a growth model in which college attainment and wealth inequality rise together. I distinguish the effects of schooling and occupational adjustment on the top-1% wealth share from those of widening persistent return differences. The schooling experiments produce small changes in top concentration and in the contribution of widening return dispersion.

The paper also relates to quantitative accounts of U.S. wealth inequality. Hubmer, Krusell, and Smith (2021) find that declining tax progressivity is the principal driver in their quantitative account, while increased earnings risk lowers top wealth shares. My fixed-dispersion experiment produces a decline through both labor-income changes and common-return adjustment. I generate these changes in a model of computerization and quantify their contributions separately. Gomez and Gouin-Bonenfant (2024) show how lower interest rates increase wealth concentration through asset revaluations and cheaper external finance for entrepreneurs. Here, wider return dispersion induces saving and capital accumulation, which lower the common return. Concentration arises through accumulation.

The return mechanism builds on Benhabib, Bisin, and Zhu (2011) and Benhabib, Bisin, and Luo (2019), who show how heterogeneous returns generate Pareto wealth tails, addressing a limitation of standard incomplete-markets models (Stachurski and Toda, 2019). Gabaix et al. (2016) emphasize the importance of persistent differences in household growth rates for the speed of changes in top inequality. My persistence experiments examine how the duration of household return advantages affects stationary wealth concentration in general equilibrium, holding cross-sectional return dispersion fixed. The longitudinal evidence of Hubmer et al. (forthcoming) shows that matching cross-sectional concentration need not imply matching how wealthy households accumulated their wealth, underscoring the distinction between stationary distributions and accumulation dynamics.

The production block builds on the capital–skill complementarity framework of Krusell et al. (2000) and Ohanian, Orak, and Shen (2023), together with the task approach of Autor, Levy, and Murnane (2003). Its implications for occupational reallocation connect the analysis to the literature on job polarization and employment allocation across tasks (Autor and Dorn, 2013; Goos, Manning, and Salomons, 2014; Caines, Hoffmann, and Kambourov, 2017; Cortes, Jaimovich, and Siu, 2017; vom Lehn, 2020; Jaimovich and Siu, 2020).

Section 2 presents the model, and Section 3 describes its estimation and calibration. Section 4 separates the two responses to cheaper ICT, decomposes the response at fixed return premia, and reports the benchmark equilibria. Section 5 examines the roles of task bias, schooling, financing, and return persistence, and Section 6 presents the robustness exercises.

2 Model

Time is discrete. The economy consists of a representative competitive final-good firm and a continuum of households of unit mass, with a perpetual-youth demographic structure. The quantitative analysis compares stationary equilibria for 1967, 1979, 1999, and 2019, using the measured price of computer capital, p_c, together with benchmark-specific ICT depreciation rates and education costs.

2.1 Production

The final good is produced with a nested-CES technology in the tradition of Krusell et al. (2000). Let K_s denote structural (non-ICT) capital, K_c computer (ICT) capital, and L_a, L_r, and L_m the efficiency-unit supplies of abstract, routine, and manual labor. Output is

$$Y = Z\, K_s^{\alpha}\, M^{\gamma}\, L_m^{1-\alpha-\gamma}, \tag{1}$$

where Z is neutral total factor productivity, normalized to one and held fixed across benchmark years in the baseline. The Cobb–Douglas outer layer combines structural capital, a non-manual composite M, and manual labor. The composite M combines routine labor with a bundle G of abstract labor and computer capital,

$$M = \left[\mu\, L_r^{\sigma} + (1-\mu)\, G^{\sigma}\right]^{1/\sigma}, \qquad G = \left[\xi\, L_a^{\lambda} + (1-\xi)\, K_c^{\lambda}\right]^{1/\lambda}, \tag{2}$$

where μ is the weight on routine labor in M, and ξ is the weight on abstract labor in G.

Two substitution elasticities govern the task response to computerization. The elasticity between routine labor and the abstract–computer bundle is $1/(1-\sigma)$, while the elasticity between abstract labor and computer capital is $1/(1-\lambda)$. An elasticity above one between routine labor and the

bundle facilitates substitution away from routine labor as computer capital becomes cheaper. The ordering $\lambda < \sigma$ makes the inner-nest elasticity smaller, capturing the relative complementarity between abstract labor and computer capital. This is the capital–skill complementarity condition of Krusell et al. (2000), applied here to task groups. I estimate both elasticities by GMM using task and ICT data; Section 3.2 reports the estimates and Appendix A describes the estimation procedure.

The Cobb–Douglas outer layer implies a unit elasticity of substitution among structural capital, the non-manual composite, and manual labor. Structural capital receives a gross income share of α, while computer capital's income share varies with the composition of the non-manual bundle.

Wages and capital rental rates equal marginal products, with labor paid per efficiency unit. Households own both types of durable capital through a single diversified claim. Aggregate household net worth A finances the structural and computer capital stocks:

$$A = K_s + p_c K_c, \tag{3}$$

where p_c is the price of ICT capital relative to the final good, and the price of non-ICT capital is normalized to one. No-arbitrage equates the net returns on the two capital stocks:

$$r + \delta_s = \frac{\partial Y}{\partial K_s}, \qquad r + \delta_c = \frac{1}{p_c}\frac{\partial Y}{\partial K_c}, \tag{4}$$

where r is the common net return and δ_s and δ_c are the depreciation rates of structural and computer capital, respectively.[3] Within each stationary equilibrium, p_c is constant, so net returns equal rental yields less depreciation. The historical no-arbitrage condition used in the GMM estimation also incorporates changes in the ICT price (Appendix A).

Given aggregate household wealth and labor supplies, equations (3) and (4) jointly determine the allocation of wealth across the two capital stocks and the common return.[4] Combining (1) and (4) gives $r = \alpha Y/K_s - \delta_s$, linking the common return to the structural-capital–output ratio. A higher K_s/Y therefore corresponds to a lower common return.

[3] Structural capital depreciates at $\delta_s = 0.05$. The benchmark-specific ICT depreciation rates come from the capital series used in the production estimation, rising from approximately 0.14 in 1967 to 0.18 in 2019.

[4] In the calibrated economy, ICT accounts for 6.0–7.3% of the value of the two-capital aggregate $K_s + p_c K_c$ across the four benchmarks, compared with a measured range of 6.3–9.1% for the corresponding aggregate. These shares are not targeted.

A decline in p_c encourages the use of computer capital. Under the capital–skill complementarity structure described above, this shifts relative labor demand toward abstract tasks and away from routine tasks, changing task wages and households' occupational choices.

2.2 Households

Households are heterogeneous in a lifetime *routine-efficiency* type η and a persistent *return* type ω, as well as in idiosyncratic labor productivity z, asset holdings a, and education status. The routine-efficiency type remains fixed throughout life, while the return type is redrawn with probability p_{ref} in each period that the household survives. Both types are redrawn at death. Labor productivity z follows a Markov process. Households have CRRA preferences over consumption and discount future utility by β.

Demographics. Each period, a household dies with probability p_{die} and is replaced by a newborn who inherits the deceased household's assets and labor-productivity state. The newborn draws new routine-efficiency and return types (η', ω') and chooses whether to attend college. Households value their descendants' utility, so saving also reflects the schooling options available to the next generation. This perpetual-youth structure (Blanchard, 1985) maintains a constant population while allowing household types and education to change across generations.

Skills, occupations, and education. Education and occupation are distinct choices. Education is chosen once at birth and affects a household's productivity, while occupational sorting takes place each period according to comparative advantage across the three tasks. This distinction matters empirically: in 1967, about 13% of workers held a college degree, whereas about 26% worked in abstract occupations. The model therefore allows non-college workers to perform abstract tasks.

A college household supplies abstract labor at efficiency κ and earns $w_a \kappa z$, where $w_a = \partial Y / \partial L_a$ is the abstract wage per efficiency unit. A non-college household chooses the task that maximizes its labor income:

$$y_U(\eta, z) = \max \left\{ \underbrace{w_r \eta}_{\text{routine}}, \underbrace{w_m}_{\text{manual}}, \underbrace{w_a b_{nc} \eta^{\rho}}_{\text{abstract}} \right\} z, \tag{5}$$

where w_r and w_m are the routine and manual wages per efficiency unit. For non-college households,

efficiency is normalized to one in manual work, equals η in routine work, and equals $b_{nc}\eta^{\rho}$ in abstract work. The parameter $b_{nc} < \kappa$ sets the scale of non-college abstract efficiency, while $\rho > 1$ makes abstract work increasingly attractive relative to routine work as η rises. In the calibrated economy, low-η non-college workers choose manual tasks, intermediate-η workers choose routine tasks, and high-η workers choose abstract tasks.

As computerization raises w_a relative to w_r, the cutoff between routine and abstract work falls, drawing more non-college workers into abstract tasks. Manual work also becomes more attractive relative to routine work at the lower end of the η distribution. These changes in relative wages generate task polarization through households' occupational choices.

Education is chosen at birth. Let v_U and v_S denote the values of non-college and college households, respectively, and let $\underline{a}$ denote the borrowing limit. A newborn with state (a', η', ω', z') compares the value of entering as non-college with the value of paying the schooling cost ϕ and entering as college. Schooling is financed from inherited assets, so enrollment requires $a' - \phi \geq \underline{a}$. For households that satisfy this constraint, the value advantage of college is

$$\Delta v(a', \eta', \omega', z') = v_S(a' - \phi, \omega', z') - v_U(a', \eta', \omega', z'), \tag{6}$$

and the probability of enrollment increases with this advantage.[5] Changes in task wages affect the relative value of college and non-college work, while inherited wealth determines whether the schooling cost can be financed. College attainment therefore responds to both schooling incentives and affordability.

Assets and returns. Households earn a gross return $1 + r + \widehat{\omega}$ on positive net worth, while borrowing carries the common interest rate r. Asset holdings lie in $[\underline{a}, \bar{a}]$; the benchmark sets $\underline{a} = 0$. The budget constraint is

$$a' = (1 + r + \widehat{\omega}\,\mathbf{1}\{a \geq 0\})\, a + y(h, \eta, z) - \tau - c, \qquad \underline{a} \leq a' \leq \bar{a}, \tag{8}$$

[5] Independent extreme-value taste shocks to the two education options, each with scale ϑ, give the college-entry probability

$$\Pr(\text{college} \mid a', \eta', \omega', z') = \frac{1}{1 + \exp(-\Delta v/\vartheta)}, \tag{7}$$

for households able to finance tuition; otherwise, the probability is zero. Section 3.3 reports the choice of ϑ and the sensitivity of the results to it.

where h denotes education status, $y(h, \eta, z)$ is labor income from the household's task, c is consumption, τ is a uniform lump-sum tax defined below, and $\widehat{\omega}$ is the household's return premium, defined in (9). The primitive return type ω has mean zero across households. Persistent differences in returns allow households with sustained return advantages to compound their wealth and accumulate disproportionately.

The return-dispersion channel. I allow the dispersion of household return premia to rise with the stock of computer capital. Let K_c denote equilibrium computer capital and K_c^{ref} its 1967 value. Each household's return premium is scaled as

$$\widehat{\omega}(\omega, K_c) = \omega \left(K_c / K_c^{\text{ref}} \right)^{\psi}, \tag{9}$$

where $\psi \geq 0$ is the elasticity of the standard deviation of return premia with respect to computer capital. The normalization leaves the 1967 return distribution unchanged. With the channel inactive ($\psi = 0$), $\widehat{\omega} = \omega$: households retain their persistent return differences at the initial dispersion. With the channel active ($\psi = \psi^\star > 0$), computer-capital accumulation widens these differences. This ICT-linked rule scales the return premia while leaving the return-type refresh process unchanged.

Financing return premia. Household return premia are financed by a uniform lump-sum tax. The aggregate premium bill is

$$L = \int_{a \geq 0} \widehat{\omega}(\omega, K_c)\, a \, d\nu,$$

where ν denotes the household distribution. With a unit mass of households, setting $\tau = L$ balances the premium bill and leaves aggregate capital income net of the tax equal to rA. Return premia therefore redistribute capital income across households. By affecting household saving and the wealth distribution, they also change aggregate capital and equilibrium factor prices.

The wealth-weighted mean total return before the financing tax is

$$\bar{r}_W = \frac{\int (r + \widehat{\omega}) a \, d\nu}{A} = r + \frac{L}{A} = r + \frac{\tau}{A}. \tag{10}$$

Both r and $\bar{r}_W$ are net of depreciation. In the calibrated economy, high-return households hold

more wealth, so the wealth-weighted premium is positive even though its mean across households is zero. After financing payments are deducted across all households, aggregate capital income per unit of wealth remains r.

2.3 Stationary equilibrium

For given benchmark inputs, a stationary recursive competitive equilibrium consists of household value and policy functions, a stationary distribution ν over (a, h, η, ω, z), factor prices, a lump-sum tax τ, and capital stocks (K_s, K_c) such that households and the firm optimize; the no-arbitrage conditions (4) hold; the capital market clears, with household net worth financing both stocks, $A = K_s + p_c K_c = \int a \, d\nu$; labor markets clear with efficiency-unit supplies (L_a, L_r, L_m) determined by household choices; the lump-sum tax balances the return-premium budget; and ν is invariant under household policies, productivity shocks, return-type refresh, and the death-and-rebirth process.

2.4 Solution method

I solve for equilibrium by iterating on labor supplies (L_a, L_r, L_m), aggregate household wealth A, and the lump-sum tax τ. At each step, the firm's first-order conditions and the no-arbitrage conditions determine the allocation of wealth across the two capital stocks and the associated factor prices. Saving is a continuous choice, and occupation cutoffs and tuition affordability are integrated within type bins and asset-grid cells. I report the allocation averaged over the final iterations, compute prices there, and re-evaluate household decisions and the stationary distribution to check market clearing. Appendix C describes the algorithm, the numerical acceptance criteria, and the treatment of the upper tail.

3 Estimation and Calibration

3.1 Preferences and benchmark inputs

A period is one year. Table A.2 in Appendix D reports parameter values, data sources, and calibration targets. Preferences are CRRA with risk aversion 1.5 and discount factor $\beta = 0.96$. The death probability is $p_{\text{die}} = 0.0222$, corresponding to an expected working life of about 45 years.

Idiosyncratic productivity z takes two values $\{0.4, 1.0\}$ with a symmetric persistence-0.8 Markov chain. Structural capital depreciates at $\delta_s = 0.05$. The price of computer capital falls by a factor of roughly 385 along its measured 1967–2019 path; the series is a quality-adjusted relative price of ICT capital, constructed as in DiCecio (2009).

The baseline holds the neutral productivity level at its measured 1967 value, normalized to one in model units; output varies with equilibrium inputs.[6] The measured relative price of ICT capital is converted to model output units using the factor implied by this normalization (1.23), so the 1967 model economy uses the measured ICT price under the estimated technology. Holding neutral productivity fixed separates the effects of the benchmark inputs from neutral productivity growth over the period.

Two other inputs change across the benchmark years. The ICT depreciation rate δ_c is measured from the capital series used in estimation (0.142 in 1967, 0.179 in 2019). The education cost follows $\phi_t = \phi_{1967} R_t^{\chi}$, where R_t is a college tuition-to-income index relative to its 1967 value (1.00, 0.89, 1.30, and 1.67 in the four benchmark years), and $\chi = 0.30$ is the pass-through, which is calibrated with the later path of college attainment in view. Section 5 reports experiments holding these inputs at their 1967 values.

3.2 The production block

The production block has six estimated parameters: the structural-capital share α, the non-manual composite share γ, the CES weights μ and ξ, and the substitution exponents σ and λ. In Krusell et al. (2000) and Ohanian, Orak, and Shen (2023), labor is grouped by education and aggregate equipment is the complementary capital stock. I estimate all six parameters jointly by GMM using annual U.S. data on task-based labor inputs, capital stocks, and the ICT price covering 1967–2019. Abstract labor enters the estimation and the model in household efficiency units, following Ohanian, Orak, and Shen (2023), with no further scaling by the firm. The efficiency κ of a college worker is a household parameter, calibrated in Section 3.3.

The data follow Ohanian, Orak, and Shen (2023), who update the framework of Krusell et al.

[6] The labor-share and wage-bill moments used to estimate production parameters are invariant to a common multiplier, while the no-arbitrage moment uses observed output. At given inputs, the multiplier leaves relative task wages and factor shares unchanged. In general equilibrium, it affects saving, capital, tuition affordability, and the common return. Since return dispersion depends on K_c, neutral growth can also widen it without a change in the ICT price. Section 6 reports the measured-productivity counterfactual; Table A.20 in Appendix D also reports a local sensitivity.

(2000) through 2019. The sample covers the pre-pandemic computerization period. Capital stocks are constructed by perpetual inventory from NIPA investment series with time-varying depreciation. Task-based labor inputs and wage bills are calculated from the Current Population Survey (Flood et al., 2025) using the methodology described in Ohanian, Orak, and Shen (2023). I classify each occupation by the task in which its measured intensity is highest, following Autor and Dorn (2013). The relative price of ICT capital proxies the inverse of investment-specific technical change.

I use four moment conditions to estimate the production block: a historical no-arbitrage condition for returns on structural and ICT capital, the aggregate labor share, the abstract-to-routine wage-bill ratio, and the manual-to-routine wage-bill ratio, which is available under the three-task classification. The baseline specification instruments each moment with a constant, the two capital stocks, and the ICT price, and uses two-step GMM with a Newey–West HAC weighting matrix. Appendix A gives the full moment conditions and reports fit and sensitivity to richer instrument sets and an unadjusted weighting matrix; the two elasticities used by the wealth model change little across these specifications.

Table 1 reports the estimates. The elasticity between routine labor and the abstract–ICT bundle is $1/(1-\sigma) = 3.29$ ($\sigma = 0.696$), indicating substantial substitutability in the outer nest. The elasticity between abstract labor and ICT capital is $1/(1-\lambda) = 0.94$ ($\lambda = -0.068$), close to unitary. This estimate is above the original Krusell et al. (2000) value of about 0.67 and is broadly in line with later estimates, including the task-based findings of Orak (2017). Both exponents have standard errors of 0.006; the delta-method standard errors for the implied elasticities are 0.065 and 0.005. The ordering $\lambda < \sigma$ gives the technology its capital–skill complementarity, expressed here across tasks: routine labor is more substitutable with the abstract–ICT bundle than abstract labor is with ICT capital.

3.3 Household parameters

The household block includes the 1967 education cost ϕ, college efficiency κ, the non-college abstract-efficiency scale b_{nc}, routine-efficiency dispersion σ_η, and the education taste parameter ϑ. I calibrate ϕ, κ, and b_{nc} jointly to three moments in the 1967 U.S. cross-section: the college share of employed workers, the abstract share of abstract-plus-routine labor in efficiency units, $L_a/(L_a + L_r)$,

Table 1: GMM estimates of the production block

Parameter	Estimate	Std. err.	Implied elasticity
α (structural-capital share)	0.267	0.002	–
γ (non-manual composite share)	0.692	0.002	–
$1-\alpha-\gamma$ (implied manual share)	0.041	–	–
μ (routine CES weight)	0.339	0.001	–
ξ (abstract CES weight)	0.904	0.001	–
σ (outer-nest exponent)	0.696	0.006	$1/(1-\sigma) = 3.29$
λ (inner-nest exponent)	−0.068	0.006	$1/(1-\lambda) = 0.94$

Note: Two-step GMM with a Newey–West HAC weighting matrix (Bartlett kernel, three lags) and four instruments in levels $\{1, K_c, K_s, p_c\}$, yielding 16 moments for six estimated parameters. Reported standard errors are HAC robust. Hansen $J = 10.9$ (10 degrees of freedom, $p = 0.36$).

and the share of workers employed in abstract tasks, respectively. Since schooling and occupation are distinct choices, the college share and abstract-task employment share discipline different parameters, ϕ and b_{nc}. I hold the remaining shape parameters at the benchmark values $\rho = 1.5$ and $\sigma_\eta \simeq 0.20$. The curvature $\rho > 1$ gives higher-η workers a comparative advantage in abstract tasks, while σ_η governs the dispersion of log routine efficiency. The education taste parameter ϑ is set separately below.

These parameters are calibrated jointly with return persistence, which targets the 1967 top-1% wealth share (Section 3.4). Table 2 reports the four targets and additional moments. All three labor-market targets and the initial top-1% share are matched with high precision. The later benchmarks retain this calibration, with the education cost evolving according to the tuition rule above. Section 6.5 describes the recalibration under the alternative return distribution, while Appendix C describes the numerical procedure.

I use a small taste-shock scale, $\vartheta = 0.02$, which smooths college entry around the cutoff. For almost all newborns, the value difference between college and no college is large relative to ϑ, so schooling is determined primarily by economic incentives and tuition affordability. The reported changes are insensitive to the precise taste scale: re-solving the 1967 and 2019 economies with $\vartheta = 0.01$ and 0.04 changes the 1967–2019 rise in the top-1% wealth share by less than 0.01 percentage points and the rise in the college share by less than 0.02 percentage points.

The routine and manual employment shares and task wage premia are additional model outcomes. The routine employment share is 65.0%, compared with 64.3% in the data, and the manual share is 8.8%, compared with 9.5%. The abstract-to-routine wage ratio per efficiency unit is

Table 2: The 1967 equilibrium: calibration targets and additional moments

Moment	Model	Target/data
Household calibration: ϕ, κ, and b_{nc}		
College share of employed workers	13.1	13.1
Abstract efficiency share, $L_a/(L_a + L_r)$	36.0	36.0
Abstract-task employment share	26.2	26.2
Return-persistence calibration: p_{ref}		
Top-1% wealth share (%)	27.64	27.66
Non-targeted moments		
Routine-task employment share	65.0	64.3
Manual-task employment share	8.8	9.5
Abstract efficiency share, $L_a/(L_a + L_r + L_m)$	33.1	34.0
Abstract/routine wage, w_a/w_r	1.15	1.10
Manual/routine wage, w_m/w_r	0.77	1.07
Abstract/routine wage bill	0.648	0.615
Local Pareto slope, top 1–0.1%	1.35	–
Top-10% wealth share	55.6	69.3
Net return r (%)	2.01	2–4

Note: Shares are percentages. The three household parameters and the refresh rate are calibrated jointly, with routine-efficiency dispersion σ_η and abstract-efficiency curvature ρ held fixed. The refresh rate targets the 1967 top-1% share; the local Pareto slope is a model outcome. Labor and schooling data are described in Section 3.2; wealth shares are from the World Inequality Database. Wages are per efficiency unit, and wage bills equal wages times efficiency-unit inputs.

1.15, compared with 1.10 in the data.

3.4 Calibrating the return channel

The return channel has three components: the 1967 level of return dispersion, the persistence of the return type, and the elasticity ψ linking dispersion to computer capital. Each is calibrated to a separate moment or relationship. The fixed-dispersion benchmark ($\psi = 0$) retains the calibrated initial dispersion and persistence.

Level. The baseline uses a mean-zero Normal distribution for ω. I set the 1967 dispersion of the persistent return type so that the model's cross-sectional standard deviation of returns to wealth is 6.0 percentage points. This matches the persistent (household fixed-effect) component of returns to net worth estimated by Fagereng et al. (2020) using Norwegian administrative data, which is 6.02 percentage points before tax.[7] The model's return type captures this persistent component and is redrawn with probability p_{ref} during survival.

[7] Panel A of Table 7 in Fagereng et al. (2020); their small-sample-corrected estimate is 5.21 percentage points.

Persistence. I set the refresh rate p_{ref} to match the 1967 top-1% wealth share in the World Inequality Database, 27.66%. The model share is 27.64% at $p_{\text{ref}} = 0.198$, implying an expected return-type duration of 4.64 years.[8] The local Pareto slope over the top 1–0.1% of the wealth distribution is 1.35. Table A.3 in Appendix D reports an alternative calibration that targets the local tail slope.

Growth. Given the calibrated level and persistence, the elasticity ψ in equation (9) determines how the rise in computer capital affects return dispersion. I calibrate ψ to match the 1967–2019 increase in the top-1% share of net personal wealth among equal-split adults reported by the World Inequality Database (2022): 7.2 percentage points, from 27.66% to 34.85%. The calibrated value, $\psi^\star = 0.0441$, reproduces this increase to within 0.02 percentage points. Figure A.1 in Appendix D shows the calibration and equilibrium response. As ψ rises, the 2019 top-1% share increases while the common return falls. At $\psi = \psi^\star$, the common return is 0.86%. Wider dispersion raises saving by high-return households, deepens capital, and lowers the common return. The initial wealth-share level and its subsequent increase are calibration targets; the top-10% share, other wealth shares, intermediate-year cross-sections, and the return-by-wealth gradient are additional model outcomes.

Evidence and interpretation. Equation (9) links computer-capital accumulation to the dispersion of persistent household returns. Administrative studies document persistent heterogeneity in returns, with particularly wide dispersion for private business wealth (Fagereng et al., 2020; Bach, Calvet, and Sodini, 2020).

One mechanism operates through firm scale and profitability. Bessen (2020) links proprietary IT to rising industry concentration, with disproportionate gains in market share for leading firms. Using French firm data, Lashkari, Bauer, and Boussard (2024) show how falling IT prices can increase returns to scale and concentration. Calligaris, Criscuolo, and Marcolin (2018) find higher markups in digitally intensive sectors and a widening gap relative to other sectors. These findings complement evidence of widening dispersion in returns on invested capital (Furman and Orszag, 2015), markup growth concentrated among high-markup firms (De Loecker, Eeckhout, and Unger, 2020), and stronger productivity divergence in ICT-intensive services (Andrews, Criscuolo, and Gal, 2016).

[8] A return-type spell ends at death or refresh, so its expected duration is $[p_{\text{die}} + (1 - p_{\text{die}})p_{\text{ref}}]^{-1}$.

A second mechanism operates through investment expertise. Kacperczyk, Nosal, and Stevens (2019) show in a portfolio-choice model that improvements in information processing disproportionately benefit sophisticated investors and increase capital income inequality. Innovation can also distribute gains unevenly between owners of new and existing businesses (Kogan, Papanikolaou, and Stoffman, 2020; Gârleanu, Kogan, and Panageas, 2012).

These mechanisms motivate a positive link between computer capital and persistent household return dispersion. The model's premium provides a reduced-form representation of the persistent household advantages that can arise from these business and investment channels. Ownership and portfolio composition mediate this link.[9] The evidence guides the economic interpretation of the rule; its household-level elasticity remains calibrated to the wealth-share increase. The calibrated ψ measures the widening of persistent return advantages required to reproduce that increase, given the model's other responses to computerization.

At $\psi^\star$, computer capital is 801 times its 1967 level. Equation (9) implies that the standard deviation of persistent returns rises by a factor of $801^{\psi^\star} \approx 1.34$, from 6.0 to about 8.1 percentage points, an increase of about one-third. This is the change in the persistent component of returns; the cross-sectional dispersion of realized returns also reflects transitory variation.

Return-by-wealth gradient. Because households with higher persistent return types accumulate more wealth, the model generates a positive relationship between returns and wealth. Bach, Calvet, and Sodini (2020) provide an external benchmark from Swedish administrative data: returns for the top decile and top percentile exceed the median by +1.14 and +2.53 percentage points, respectively. In the 2019 model, the corresponding gaps are +3.4 and +3.3 percentage points. Persistent return advantages generate a premium for wealthy households that is similar across these two groups in the model. In the Swedish data, the premium rises from the top decile to the top percentile. Portfolio composition and asset scale also contribute to that empirical gradient.

[9] Unincorporated business and real estate declined as a share of the top percentile's assets between 1983 and 2019 (Wolff, 2021).

4 Quantitative results

Computerization affects top wealth concentration through two opposing responses in the model. With return premia held fixed, cheaper ICT changes wages, schooling, and capital accumulation in ways that lower top concentration. Under the calibrated ICT-linked rule ($\psi = \psi^\star$), the resulting expansion of computer capital also widens persistent return differences, more than offsetting this decline. I first separate these responses, then relate them to the historical benchmark equilibria.

4.1 Computerization and wealth concentration

To isolate the ICT-price effect, I compare economies at the measured 1967 and 2019 prices, keeping ICT depreciation and education costs at their 2019 values. I make this comparison under two fixed distributions of persistent return premia: the initial distribution, denoted F_{67} and retained when $\psi = 0$, and the wider distribution generated by the baseline 2019 economy at $\psi = \psi^\star$, denoted F_{19}. Their standard deviations are 6.00 and 8.06 percentage points. For these price comparisons, I impose each distribution and hold it fixed as computer capital changes. Wages, the common return, the financing tax, saving, schooling, and the stationary wealth distribution adjust.

Panel A of Figure 1 shows that cheaper ICT reduces top wealth concentration under both premium distributions. At F_{67}, the top-1% share falls from 29.00% to 20.86%, a decline of 8.14 percentage points. At F_{19}, it falls from 43.45% to 34.84%, or 8.61 points. Holding the ICT price fixed, widening premia from F_{67} to F_{19} raises the top-1% share from 29.00% to 43.45% at the 1967 price, an increase of 14.45 percentage points. At the 2019 price, the same widening raises the share from 20.86% to 34.84%, an increase of 13.98 points. Cheaper ICT therefore dampens the effect of widening premia by 0.47 percentage points, the difference between these two increases.

Cheaper ICT raises labor incomes and expands both capital stocks (Table 3). The three task wages rise by roughly 53–63%, the common return falls by 0.24–0.30 percentage points, and mean wealth roughly doubles. Median wealth rises more than mean wealth. Employment shifts strongly out of routine tasks: the abstract share rises by about 33–34 percentage points, and college attainment rises by 21–25 points. These changes show how computerization can polarize employment while reducing top wealth concentration.

Panel B restores the link between computer capital and return dispersion in equation (9), with

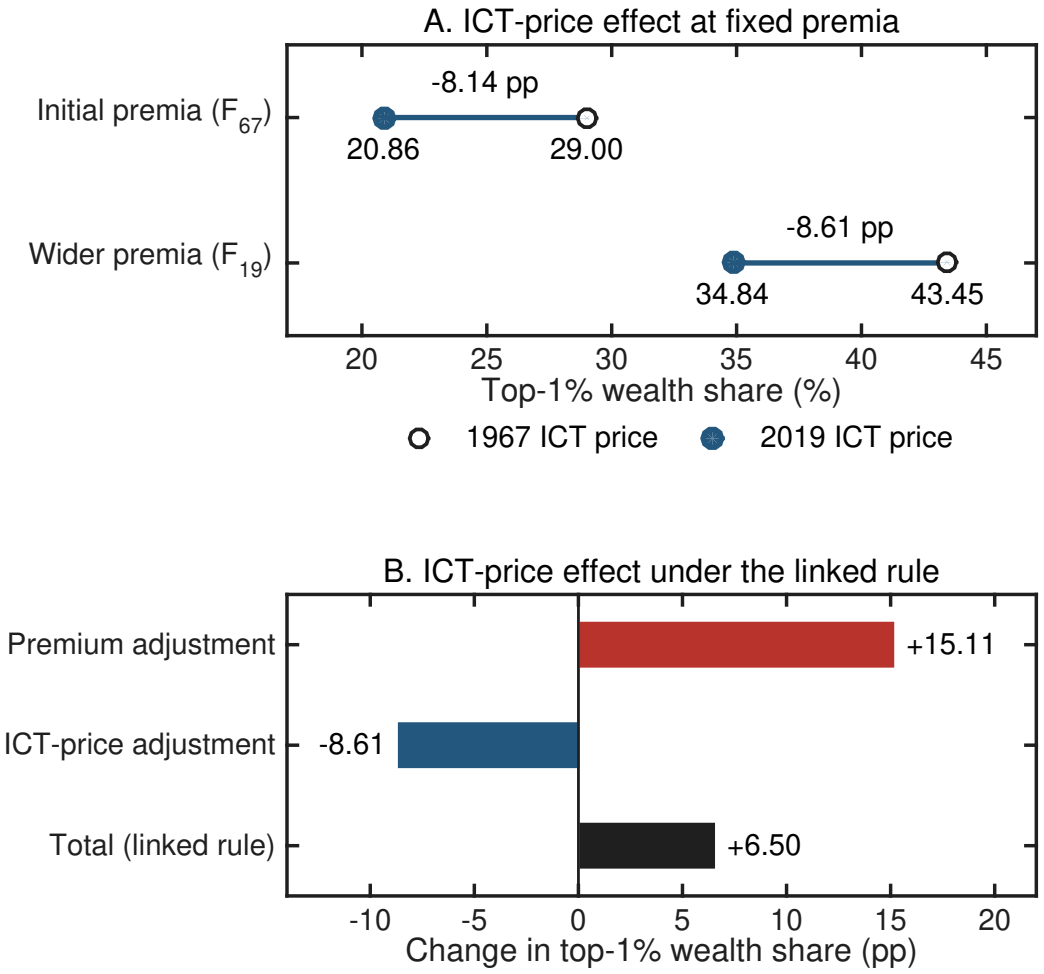


Figure 1: Computerization and wealth concentration

Note: Each panel compares stationary equilibria at the 1967 and 2019 ICT prices, with 2019 tuition and depreciation. Panel A fixes premia at F_{67} (initial dispersion, $\psi = 0$) or F_{19} (the baseline 2019 distribution). Panel B decomposes the price effect under the ICT-linked rule ($\psi = \psi^{\star}$): first impose F_{19} at the old price, then lower the price with F_{19} fixed. The two adjustments sum to the 6.50-percentage-point increase.

Table 3: Economic responses to cheaper ICT

	Initial premia F_{67}	Wider premia F_{19}
Common return r (pp)	−0.30	−0.24
Total return $\bar{r}_W$ (pp)	−0.37	−0.32
Lump-sum premium tax τ (%)	+93.4	+91.6
relative to lowest labor income $w_m z_\ell$ (pp)	+3.79	+7.77
Mean wealth (%)	+103.5	+97.9
Median wealth (%)	+137.3	+129.3
College attainment (pp)	+24.59	+21.30
Abstract-task employment (pp)	+33.75	+33.38
of which non-college (pp)	+9.16	+12.08
Routine-task employment (pp)	−35.27	−34.80
Manual-task employment (pp)	+1.52	+1.43
Abstract wage w_a (%)	+62.3	+62.9
Routine wage w_r (%)	+53.6	+52.8
Manual wage w_m (%)	+63.1	+60.9
Output Y (%)	+91.8	+87.5

Note: Each column compares the 2019 ICT price with the 1967 price at a fixed premium distribution and 2019 tuition and depreciation. Household choices and equilibrium prices adjust. Total return $\bar{r}_W$ is wealth-weighted and includes premia before the financing tax; both return measures are net of depreciation. The lowest productivity state is $z_\ell = 0.4$. Wages are per efficiency unit. Employment shares count workers. Wealth statistics use the evaluated stationary distribution. pp denotes percentage points.

the return channel active ($\psi = \psi^\star$). At the 1967 ICT price, the top-1% share is 28.34%; at the 2019 price, it is 34.84%. The ICT-price decline therefore raises concentration by 6.50 points under the linked rule. This positive effect reflects the widening of persistent return differences as computer capital accumulates.

Starting from the old-price economy under the linked rule, I first replace its premium distribution with F_{19} while keeping the ICT price fixed. This raises the top-1% share by 15.11 points. Lowering the ICT price with F_{19} held fixed then reduces the share by 8.61 points, leaving the net increase of 6.50 points.[10] Under the calibrated relationship, wider return opportunities more than offset the equalizing effect of cheaper ICT at fixed premia.

This price experiment holds depreciation and tuition at their 2019 values throughout. The historical benchmark comparison also changes those two inputs and targets the observed 7.2-point wealth-share increase. The 6.50-point effect measures the ICT-price decline with dispersion

[10]With the ICT price held at its 1967 value and the other inputs at 2019 values, the linked rule gives a premium standard deviation of 5.92 points and computer capital of 0.728 times its actual 1967 value. The premium adjustment in this decomposition therefore starts from a slightly narrower distribution than F_{67}. At the 2019 price, the imposed F_{19} and linked-rule solutions coincide at the displayed precision. Table A.4 reports the complete set of equilibria.

responding through the linked rule ($\psi = \psi^\star$). The 13.98-point effect measures widening premia from F_{67} to F_{19} at the same 2019 inputs.

4.2 Wages, the common return, and the financing tax

Table 4 separates the ICT-price effect at fixed premia into changes in the three task wages and changes in the common return together with the lump-sum financing tax. For each premium distribution, I start from the equilibrium at the 1967 ICT price and replace one set of prices with its values at the 2019 price. Household choices and the stationary distribution respond, while the specified wages, return, and tax remain fixed. Tuition remains at its 2019 value throughout.

Both adjustments lower top concentration under both premium distributions. I report each block's contribution averaged across the two possible orders of substitution. At initial premia, wages account for 2.09 percentage points of the decline and the return and tax for 6.05 points. The latter accounts for about three-quarters of the total.

Table 4: Cheaper ICT at fixed premia: wages versus the common return and tax

	Initial premia (F_{67})		Wider premia (F_{19})	
Values applied	Level (%)	Change (pp)	Level (%)	Change (pp)
Top-1% wealth share				
1967 ICT price	29.00	–	43.44	–
New wages	26.47	−2.53	38.48	−4.96
New return and tax	22.51	−6.49	39.62	−3.83
Both (2019 ICT price)	20.86	−8.14	34.84	−8.61
Wages, order average		−2.09		−4.87
Return and tax, order average		−6.05		−3.74
Interaction		+0.89		+0.18

Note: Premia, tuition, and depreciation are fixed within each column. Starting from the old-price equilibrium, the middle rows apply new-price wages or the new-price common return and tax. Household choices and the stationary distribution respond at these fixed prices and tax. Changes are relative to the first row; order averages sum to the total decline. The interaction is the total change minus the two changes applied separately. Shares are single evaluations at the stated prices; small differences from Table A.4 reflect its use of window means (Appendix C).

At wider premia, the wage response contributes more: its average effect is 4.87 points, compared with 3.74 points for the return and tax. Wages therefore account for more than half of the decline. The positive interactions, 0.89 and 0.18 points, mean that each adjustment lowers concentration somewhat less after the other has occurred. These contributions include changes in saving,

occupational choice, and schooling induced by each set of prices. Appendix D.2 reports both orders and additional distributional outcomes.

4.3 Benchmark equilibria

Figure 2 compares the top-1% wealth share in the data with the model's stationary benchmark equilibria. With the return channel active ($\psi = \psi^\star$), the share rises from 27.6% in 1967 to 34.8% in 2019. The initial level and the subsequent rise are calibration targets. With dispersion fixed at its 1967 level ($\psi = 0$), the same benchmark inputs instead lower the share to 20.9%. Wider dispersion thus offsets a 6.8-point decline and produces the calibrated 7.2-point rise, giving the 13.98-point contrast at the 2019 inputs. Appendix D.3 presents a decomposition of the historical fixed-dispersion decline.

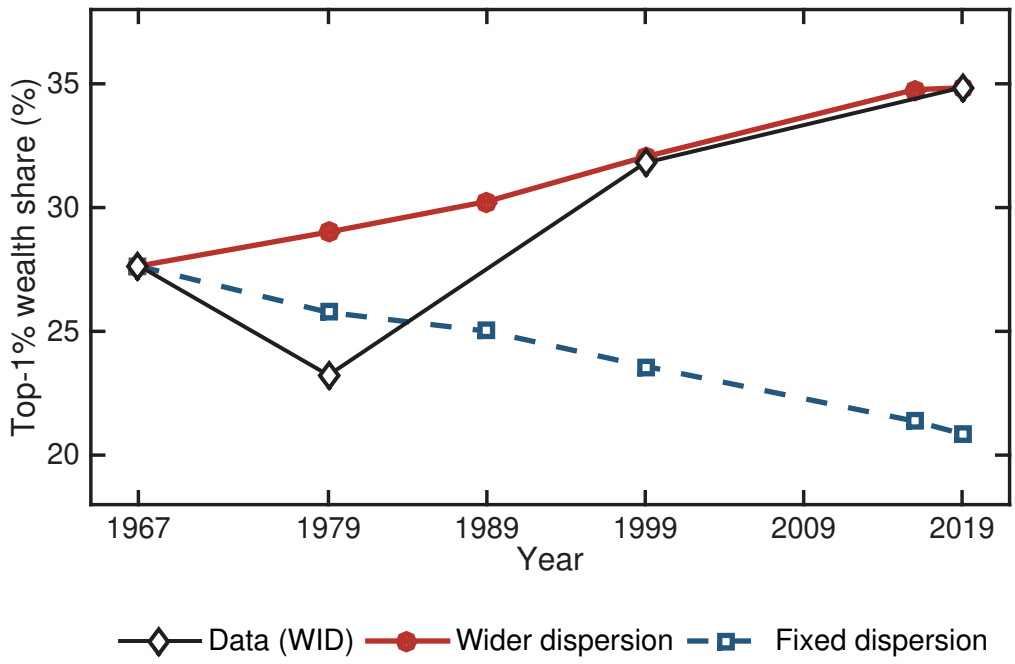


Figure 2: Top-1% wealth share, 1967–2019

Note: The channel is active when dispersion widens with computer capital ($\psi = \psi^\star$) and inactive when dispersion stays at its 1967 level ($\psi = 0$). Model points are stationary equilibria at each year's ICT price, depreciation, and education cost. Return persistence targets the initial top share and ψ the 1967–2019 increase; intermediate years, including 1989 and 2016, are model outcomes.

Table 5 reports the four benchmark equilibria with the return channel active ($\psi = \psi^\star$). I present additional distributional and task statistics in Appendix D.

Table 5: Stationary equilibria at the benchmark inputs

	1967	1979	1999	2019
Employment shares (%)				
Abstract task	26.2	34.0	46.5	58.7
Routine task	65.0	56.9	44.0	31.3
Manual task	8.8	9.1	9.5	10.0
College	13.1	19.0	22.2	29.8
Wealth distribution				
Gini coefficient	0.679	0.689	0.709	0.720
Top-1% share (%)	27.6	29.0	32.1	34.8
Top-10% share (%)	55.6	56.5	59.0	60.8
Middle-60% share (%)	28.9	28.3	26.6	25.8
Bottom-50% share (%)	9.0	8.4	7.6	7.2
Prices				
Common net return r (%)	2.01	1.77	1.37	0.86
Total return $\bar{r}_W$ (%)	3.41	3.35	3.29	3.23
Abstract/routine wage, w_a/w_r	1.15	1.17	1.22	1.25
Data comparisons				
WID top-1% share (%)	27.7	23.2	31.8	34.8
WID top-10% share (%)	69.3	65.4	68.6	71.4
College, employed workers (%)	13.1	20.1	29.4	39.2[a]
College, adults aged 25+ (%)	10.1	16.4	25.2	36.0

Note: All benchmarks use the baseline calibration and the ICT-linked return rule ($\psi = \psi^\star$). ICT prices, depreciation, and education costs vary by year. Total return $\bar{r}_W$ is wealth-weighted and includes return premia before the financing tax; both return measures are net of depreciation. Wages are per efficiency unit. The middle 60% comprises wealth percentiles 20–80 and overlaps the bottom half. Appendix C describes the reporting convention.

[a] The employed-workers series ends in 2018; this entry uses its 2018 value. WID denotes the World Inequality Database.

Polarization and schooling. The model generates labor-market polarization, with employment shifting from routine work toward abstract and manual tasks (Figure 3). Between 1967 and 2019, the routine employment share falls from 65.0% to 31.3%, while the abstract share rises from 26.2% to 58.7%. The manual share changes less, rising from 8.8% to 10.0% over the same period.

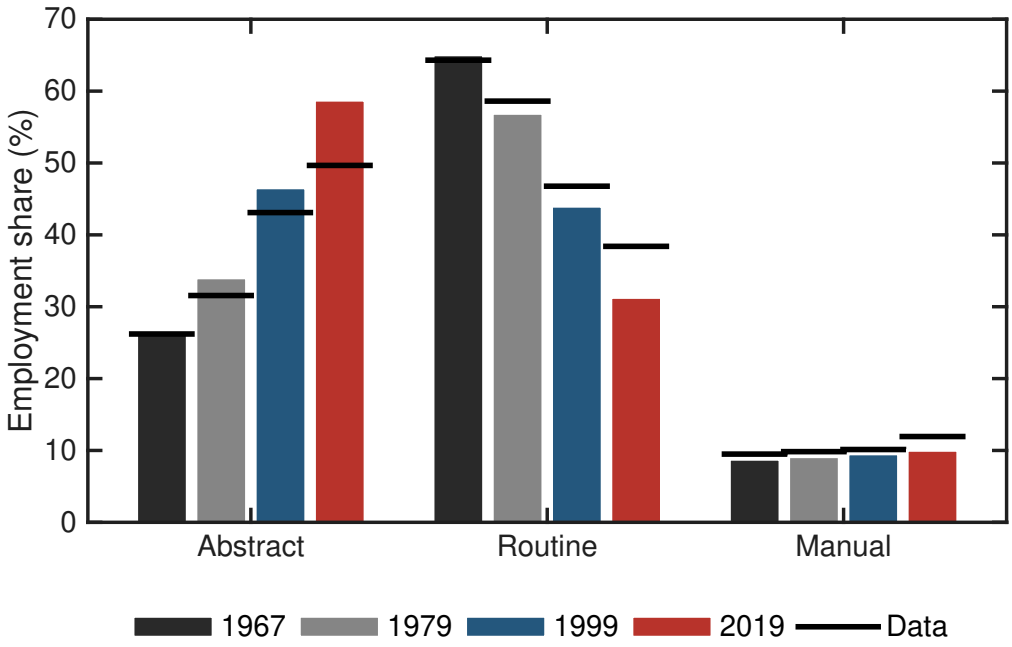


Figure 3: Employment shares by task at the four benchmark years

Note: Bars show the model's stationary-equilibrium shares of workers in each task; black ticks show the empirical task shares in the same four years. The 1967 abstract employment share is a household calibration target. The education-cost pass-through is calibrated with the later path of college attainment in view.

The college share rises from 13.1% to 29.8%, compared with 39.2% among employed workers in the 2018 data (Table 5). Greater tuition affordability explains most of the model's increase: the share of newborns who can finance college nearly doubles, from 16.5% to 32.9%, while enrollment among those who can afford it rises from 79% to 91% (Section 5). Since all college workers perform abstract tasks, the rise in college attainment accounts for about half of the increase in abstract employment. The remaining half comes from the increase in non-college abstract employment.

4.4 Wealth concentration

With the return channel active ($\psi = \psi^{\star}$), computer-capital accumulation widens the dispersion of persistent returns through equation (9), and high-return households accumulate wealth disproportionately. The upper tail thickens: the local Pareto slope over the top 1–0.1% of the wealth distribution falls from 1.35 in 1967 to 1.11 in 2019 (Figure 4; Table A.11 in Appendix D).

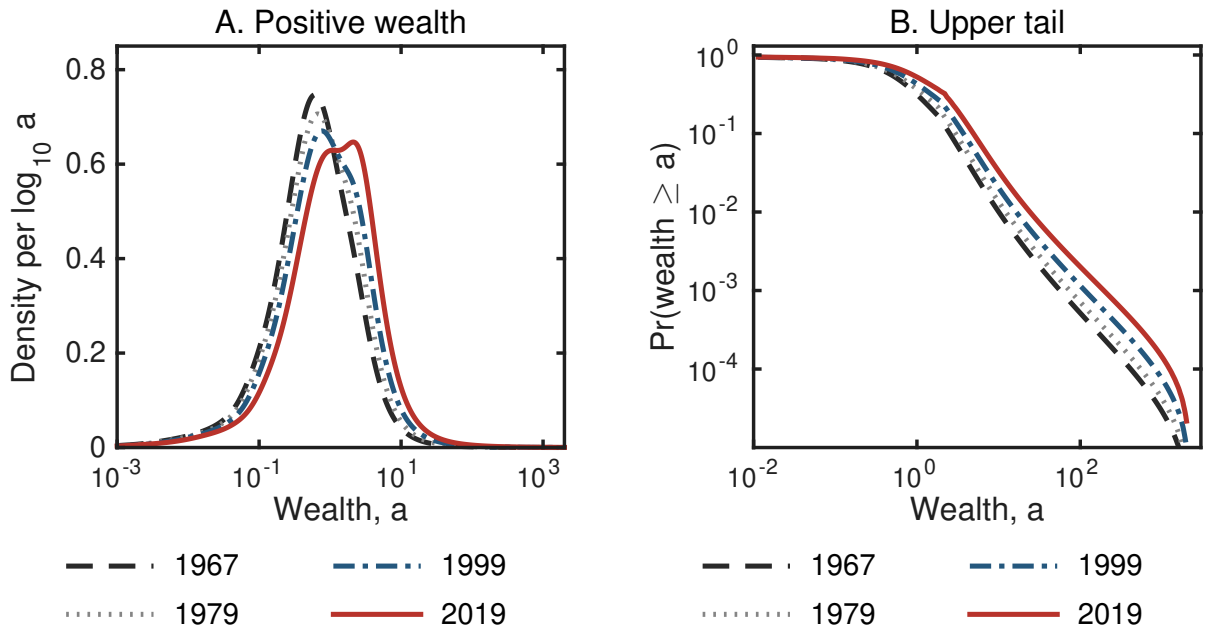


Figure 4: Stationary wealth distributions at the four benchmark years

Note: Panel A shows the density of positive wealth per decade of a, smoothed on a logarithmic axis and integrating to the share with positive wealth. The household shares at $a = 0$ are 5.36%, 5.35%, 5.45%, and 4.99% in 1967, 1979, 1999, and 2019, respectively. Panel B shows Pr(wealth $\geq a$) on logarithmic axes. A Pareto tail appears as a straight line, with a flatter slope indicating a thicker tail.

The change in the top-10% wealth share is +5.2 percentage points, compared with 7.2 points for the top 1%. The combined share of the next nine percentiles therefore falls by about two percentage points. The middle 60% and bottom half also hold smaller wealth shares in 2019 (Table 5). The model thus combines labor-market polarization with a shift of wealth toward the top percentile.

The model's 2019 top-10% wealth share is 60.8%, compared with 71.4% in the data. The top-1% share increases across the model's stationary benchmarks, while the observed share falls to 23.23% in 1979 before rising to 34.85% in 2019.

4.5 The falling common return

The common net return r falls from 2.01% in 1967 to 0.86% in 2019 as wealth becomes more concentrated. The no-arbitrage condition in equation (4) gives $r = \alpha Y/K_s - \delta_s$, so a higher structural-capital–output ratio lowers the common return. With return dispersion held at its 1967 level ($\psi = 0$), capital accumulation reduces r to 1.76% by 2019. Widening dispersion ($\psi = \psi^\star$) reinforces this effect: high-return households save more, raising aggregate wealth in 2019 by 19% relative to the fixed-dispersion economy. The additional capital accumulation lowers the common return further, from 1.76% to 0.86%.

Households' total returns also include their persistent premia. The wealth-weighted mean before the financing tax, $\bar{r}_W$ in equation (10), is 3.41% in 1967 and 3.23% in 2019 (Table 5). The 2019 fixed-dispersion economy ($\psi = 0$) gives 3.11%. Widening dispersion therefore lowers the common return while slightly raising the wealth-weighted total return before financing. The financing tax redistributes this premium income, leaving aggregate capital income per unit of wealth equal to r.

At the 2019 benchmark inputs, increasing ψ lowers the common return to zero near $\psi = 0.069$. Stationary equilibria with negative common returns are found at $\psi = 0.070$ and 0.075 (Figure A.1 and Table A.13 in Appendix D). Wider dispersion also raises the premium bill and the lump-sum tax that finances it. For a household with zero wealth, labor income must exceed this tax to permit positive consumption. The margin between the lowest labor income and the tax falls to 0.014 at $\psi = 0.075$, the last point at which a stationary equilibrium was found along this sweep. Appendix C reports the financing margins and continuation checks. Financing premia through a levy proportional to wealth leaves zero-wealth households untaxed, removing this particular constraint (Section 5).

5 Model counterfactuals

I examine how the return channel's 13.98-percentage-point effect on the 2019 top-1% wealth share depends on the task bias of technology, the financing of return premia, the schooling response, and the paths of ICT depreciation and education costs. Each counterfactual compares the 2019 top-1% share under wider return dispersion with its counterpart under the initial distribution F_{67} ($\psi = 0$). Widening either follows the ICT-linked rule ($\psi = \psi^\star$) or is imposed by fixing premia at

F_{19}, as specified below. Separate experiments vary return-type persistence while holding these cross-sectional distributions fixed. Figure 5 summarizes the main comparisons.[11] Except for the feature varied in each experiment, parameters remain at their baseline values.

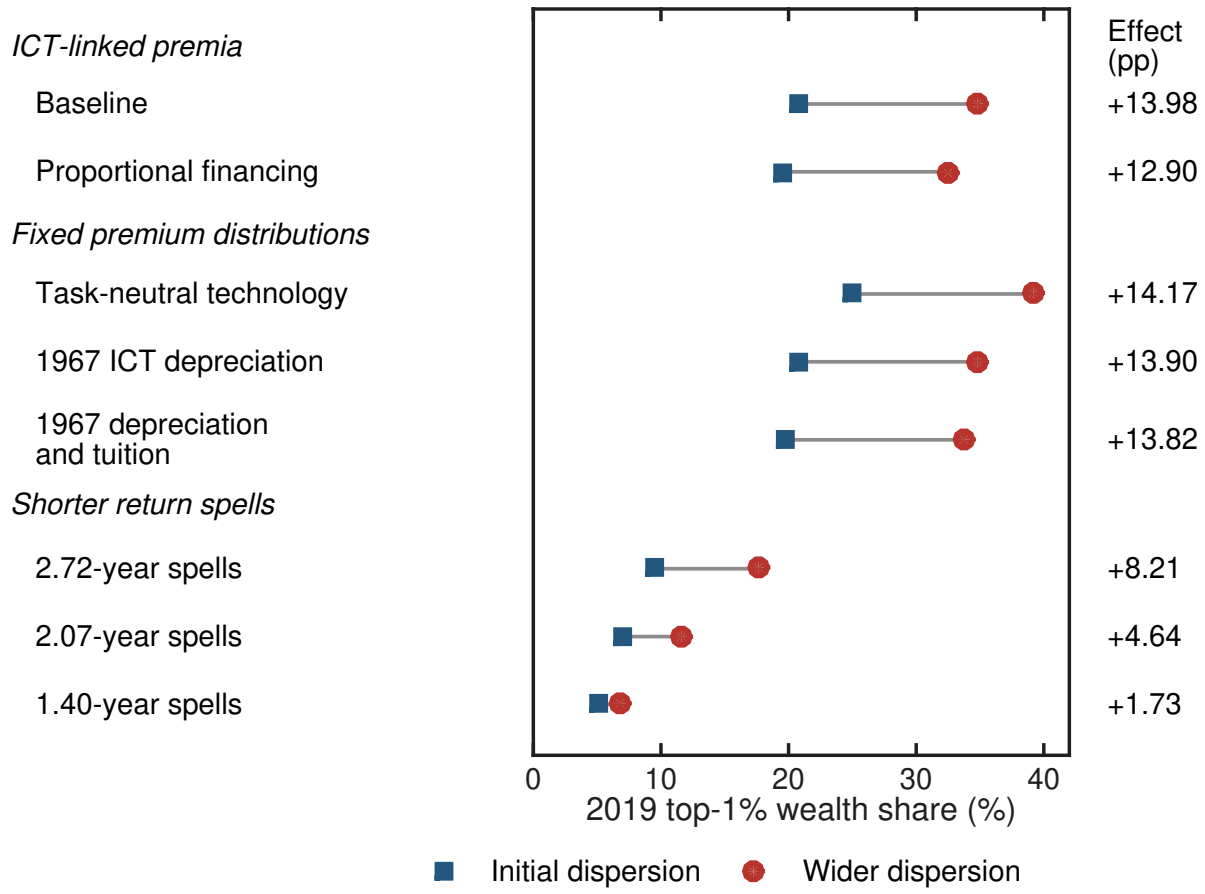


Figure 5: Counterfactual 2019 top-1% wealth shares

Note: Squares use initial dispersion and circles wider dispersion; numbers at the right give their differences in percentage points. Baseline and proportional-financing economies use the ICT-linked rule ($\psi = 0$ for squares, $\psi = \psi^\star$ for circles). The technology, depreciation, tuition, and duration experiments impose F_{67} and F_{19}. The final three rows vary return-type duration at these fixed premium distributions.

The return channel raises the 2019 top-1% wealth share by 12.9–14.2 percentage points across the baseline and the four alternative environments. The effect depends strongly on persistence: holding cross-sectional return dispersion fixed, shortening the expected duration of a return type to about two years reduces the effect to roughly one-third of its baseline value. The rest of this section

[11] Table A.14 in Appendix D reports the corresponding values.

examines each counterfactual in turn.

Task-neutral technology. The first counterfactual removes the task bias of computer capital. I replace the estimated technology with the Cobb–Douglas function tangent to it at the 1967 equilibrium, $Y = Y_0 \prod_j (X_j/X_{j0})^{s_j}$, where $X = (K_s, K_c, L_a, L_r, L_m)$, X_0 is the 1967 allocation, and s_j are the corresponding factor shares. Output and all five marginal products match the baseline at this allocation, preserving the 1967 equilibrium. Computer capital affects all task wages proportionally at given labor supplies, leaving relative task wages unchanged.[12] The comparison fixes return premia at the wider baseline 2019 distribution F_{19} or the initial distribution F_{67}. It measures how the production structure affects wealth levels and the response to the same widening of return dispersion.

Figure 5 compares the estimated technology in the baseline row with the tangent Cobb–Douglas technology in the task-neutral row. At initial premia, the estimated technology produces a 2019 top-1% share that is 4.10 percentage points lower, as shown by the difference between the two squares. At wider premia, the difference between the two circles is 4.30 points. Since both technologies reproduce the 1967 equilibrium, these are also differences in their 1967–2019 changes. Widening dispersion nevertheless has a similar effect under both technologies: 13.98 points under the estimated technology and 14.17 points under Cobb–Douglas, a difference of about 0.2 points.

With wider premia (F_{19}), the 2019 abstract-to-routine wage ratio is 1.11, compared with 1.25 in the baseline, and the college share is 19%, compared with 29.8%. The rise in college attainment since 1967 is about two-thirds smaller. Thus, removing task bias changes wage and schooling outcomes substantially while leaving a large wealth effect of persistent return dispersion.

Financing. The baseline finances return premia through a uniform lump-sum tax, so households pay the same amount regardless of their wealth. In this counterfactual, I replace this tax with a budget-balancing levy proportional to wealth, $\ell = \int \widehat{\omega} a \, d\nu / \int a \, d\nu$. Each household pays ℓa and earns a net return of $r + \widehat{\omega} - \ell$. The levy finances the return-premium bill, leaving aggregate capital income equal to rA.

The required levy is 2.5% of wealth with the channel active ($\psi = \psi^\star$) and 1.4% with dispersion

[12] The Cobb–Douglas specification imposes unit substitution elasticities among all inputs, so the experiment changes capital–labor substitution as well as task bias.

fixed ($\psi = 0$). Replacing the lump-sum tax with a wealth-proportional levy dampens the return channel's contribution by about 8%, from +14.0 to +12.9 percentage points. The financing change also affects equilibrium returns and schooling. With the channel active ($\psi = \psi^\star$), the pre-levy common return rises to about 3.3% and the college share falls to 17%.

ICT depreciation and education costs. The baseline changes ICT depreciation and education costs alongside the ICT price. I first hold depreciation at its 1967 value while using the 2019 ICT price and education cost. In the second experiment, I also hold the education cost at its 1967 value.

Each experiment compares two stationary equilibria: one with the wider baseline 2019 premium distribution F_{19} and one with the initial distribution F_{67}. Holding these distributions fixed applies the same widening of return dispersion in both experiments, even though computer capital responds to the alternative inputs.

The return channel contributes +13.9 percentage points to the 2019 top-1% wealth share when depreciation stays at its 1967 value, and +13.8 points when both depreciation and education costs stay at their 1967 values, compared with +14.0 in the baseline. Holding these inputs fixed therefore slightly dampens the return channel. The schooling response is larger: with wider return dispersion, the college share reaches 40% under F_{19} in the second experiment, compared with 29.8% in the baseline.

Schooling. College attainment rises from 13.1% to 29.8% in the baseline. Two experiments assess its role in wealth concentration (Table 6). Each compares the ICT-linked return channel ($\psi = \psi^\star$) with fixed initial dispersion ($\psi = 0$). Both restrict college entry among newborns, retain the 2019 education cost, and allow prices, saving, and the wealth distribution to adjust.[13]

The first experiment applies the 1967 college-entry probabilities to newborns in the 2019 economy, conditional on their inherited wealth, productivity, and household types. College attainment can still rise as more newborns inherit enough wealth to finance tuition. With the return channel active ($\psi = \psi^\star$), the college share is 26.5%, compared with 29.8% under the endogenous 2019 rule, while the channel's contribution to the top-1% share increases by only +0.07 percentage points. The continued expansion under the 1967 rule reflects the importance of affordability. A decomposition

[13]The restrictions apply to actual college entry. When choosing saving, households continue to value the endogenous schooling option for their descendants.

of the baseline college-entry rate attributes about 13.9 of the 16.7-percentage-point rise in attainment to the larger share of newborns able to finance tuition.

The second experiment holds college attainment at its 1967 share of 13.1%. I proportionally reduce the 2019 entry probabilities until the stationary college share reaches this target, separately with the channel active ($\psi = \psi^\star$) and with initial dispersion fixed ($\psi = 0$). Holding attainment fixed raises the 2019 top-1% wealth share by 0.03 percentage points with the channel active and lowers it by 0.47 points with dispersion fixed. The return channel's contribution therefore increases by +0.50 points. Under these entry restrictions, college expansion modestly dampens the return channel's contribution, with little effect on top concentration in the economy with the return channel active.

Table 6: College entry and wealth concentration in 2019

	College share (%)		Top-1% wealth share (%)		Return-channel contribution (pp)
College entry	On	Off	On	Off	
Endogenous (baseline)	29.8	32.6	34.8	20.9	13.98
1967 entry rule fixed	26.5	29.4	34.7	20.7	14.05
1967 college share fixed	13.1	13.1	34.9	20.4	14.47

Note: On denotes the ICT-linked rule ($\psi = \psi^\star$); off retains initial dispersion ($\psi = 0$). The final column is the on-minus-off top-share difference, using unrounded values. The first restriction applies the 1967 entry rule; the second rescales entry probabilities to maintain the 1967 college share. Both retain 2019 tuition and its affordability constraint. Prices, saving, and the wealth distribution adjust; households continue to value the endogenous schooling option for descendants.

Wider return dispersion, in turn, lowers college attainment through tuition affordability. The 2019 college share is 29.8% with the channel active ($\psi = \psi^\star$), compared with 32.6% with dispersion fixed ($\psi = 0$). A similar gap, about three percentage points, appears with the 1967 entry rule fixed. Wider dispersion raises mean wealth while reducing median wealth by about a seventh, and the share of newborns whose inherited assets fall below the tuition cost rises from 63% to 67%. This decline in affordability accounts for the lower college share; enrollment among newborns able to pay rises slightly, partly offsetting it (Table A.16 in Appendix D).

Persistence. To isolate persistence, I vary the probability that a surviving household redraws its return type, holding the cross-sectional distribution of return premia fixed. At each duration, I compare the 2019 economy under the wider premium distribution F_{19} with its counterpart under the initial distribution F_{67}. Figure 6 shows the full comparison; the last three rows of Figure 5

highlight shorter durations, and Table A.15 in Appendix D reports the values.

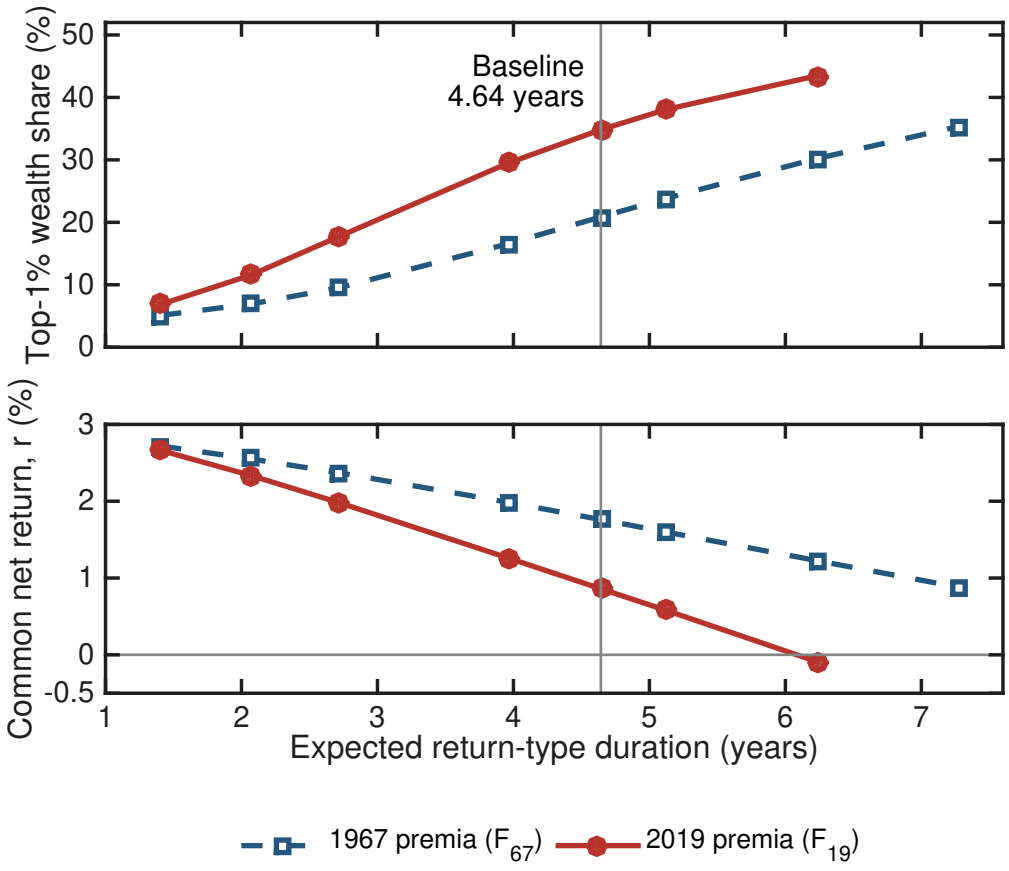


Figure 6: Return persistence and wealth concentration in 2019

Note: The panels plot the top-1% wealth share and common net return against expected return-type duration. Circles use F_{19} and squares F_{67}; these premium distributions remain fixed as the refresh probability varies. The vertical line marks the baseline duration of 4.64 years. At 7.28 years, only the fixed-dispersion equilibrium was found (Appendix C).

Shortening the expected duration of a return type from 4.64 to 2.1 years dampens the return channel substantially: its contribution to the top-1% wealth share falls from +13.98 to +4.64 percentage points, a reduction of about two-thirds. At 1.4 years, the contribution is +1.73 points. In the economy with wider dispersion, the return advantage of the top percentile over the median household also falls, from 3.3 points at the baseline duration to 0.9 points at the shortest duration. Persistent return advantages give high-return households time to accumulate wealth, making their duration central to the effect of wider dispersion.

Longer return-type durations raise wealth concentration in both economies. The return channel's

contribution reaches 14.2 percentage points at 5.1 years, then falls to 13.3 points at 6.2 years as concentration rises more rapidly in the fixed-dispersion economy. At 7.3 years, the fixed-dispersion top-1% share reaches 35.4%, compared with 20.9% at the baseline duration.[14] A given dispersion of returns can therefore support substantially different levels of wealth concentration, depending on how long return advantages persist.

6 Robustness

6.1 The asset grid

The number of asset-grid nodes controls numerical resolution, while the upper bound limits the wealth households can accumulate. Starting from the baseline grid of 300 nodes and an upper bound of 2,000, I double the number of nodes, the bound, or both, holding all calibrated parameters fixed. Table A.18 in Appendix D compares the resulting 2019 equilibria at $\psi^\star$. Saving is a continuous choice (Appendix C). Doubling the nodes leaves the top-1% share virtually unchanged at 34.8% and raises the common return by less than 0.01 percentage points, to 0.87%. Doubling the upper bound raises the share to 37.3% and lowers the common return to 0.79%. Doubling both gives the same top share at the reported precision and a common return less than 0.01 percentage points higher.

A higher asset bound raises top wealth concentration and amplifies the return channel. Table 7 compares bounds of 2,000, 4,000, 8,000, and 16,000, holding all calibrated parameters, including $\psi^\star$, fixed. Across this range, the channel's contribution rises from +14.0 to +18.1 percentage points, and the 1967–2019 increase in the top-1% share with the channel active ($\psi = \psi^\star$) rises from +7.2 to +10.3 points. The common return falls from 0.86% to 0.67%. At every bound tested, the fixed-dispersion economy ($\psi = 0$) continues to show a decline in the top-1% share between 1967 and 2019. The 1967 level is targeted at the baseline bound; with parameters unchanged, it rises from 27.64% to 31.04% over this sequence.

This sensitivity reflects substantial wealth in the far upper tail. The local Pareto slope of the highest-return type's wealth distribution is 0.85 at every bound tested (Table A.19 in Appendix D). The quantitative magnitudes are sensitive to the wealth limit over the tested range; this sequence

[14] At wider dispersion, the last solved duration is 6.23 years, with a financing margin of 0.029. No stationary equilibrium was found at 7.28 years; Appendix C describes the continuation checks.

Table 7: Wealth concentration and the upper asset bound

	Top-1% wealth share (%)			Return-channel contribution (pp)	2019 r (%)
Asset bound	1967	2019 Fixed dispersion	2019 Wider dispersion		
2,000 (baseline)	27.64	20.86	34.84	13.98	0.86
4,000	28.87	21.70	37.31	15.60	0.79
8,000	30.01	22.49	39.46	16.97	0.73
16,000	31.04	23.29	41.35	18.06	0.67

Note: Each bound uses 300 asset-grid nodes and the baseline calibration. Fixed dispersion uses $\psi = 0$; wider dispersion uses the calibrated $\psi^\star$. The return-channel contribution is the difference between the two 2019 wealth shares, calculated from unrounded values. The final column reports the common net return with wider dispersion. The 1967 share is a calibration target at the 2,000 bound only. The counterfactual comparisons in Section 5 use the baseline grid.

does not establish convergence as the limit rises. The baseline results use the bound of 2,000.

Doubling the number of asset-grid nodes raises the return channel's contribution from +14.0 to +14.1 percentage points. Using thirteen return-type nodes instead of nine changes the 1967 and 2019 top-1% wealth shares by at most 0.05 percentage points. Appendix C reports additional numerical checks.

The isolated ICT-price effects change less across bounds. At 4,000, cheaper ICT lowers the top-1% share by 8.63 points at initial premia and 8.71 points at wider premia, compared with 8.14 and 8.61 points at the baseline bound. The linked-rule price effect rises from 6.50 to 7.70 points (Table A.6 in Appendix D).

The ICT-price effects also retain their signs when return persistence targets an alternative initial tail slope. The linked-rule price effect is again 6.5 percentage points (Table A.3 in Appendix D).

6.2 The discount factor

I compare discount factors of $\beta = 0.95$ and 0.97 with the baseline value of 0.96. Figure A.2 and Table A.17 in Appendix D trace the 2019 top-1% wealth share and common return as ψ varies, holding all remaining parameters at their baseline values. At the baseline calibrated elasticity $\psi^\star$, the top-1% share is 35.7% with $\beta = 0.95$ and 33.8% with $\beta = 0.97$, compared with 34.8% in the baseline. College attainment responds more strongly: the corresponding shares are 20% and 43%, compared with 29.8%.

Greater patience encourages saving and capital accumulation, lowering the common return.

At $\psi^\star$, the return is 1.91% with $\beta = 0.95$ and −0.12% with $\beta = 0.97$, compared with 0.86% in the baseline.[15] The discount factor has a substantial effect on the common return and schooling, while the 2019 top-1% wealth share remains within about one percentage point of its baseline value at $\psi^\star$.

6.3 Neutral productivity

The baseline holds neutral productivity at its measured 1967 level. The residual implied by the estimated technology rises by a factor of 2.13 between 1967 and 2019 (Appendix A). I re-solve the 2019 economies at this measured productivity level, keeping the ICT price at its measured 2019 value in final-good units. The education cost and asset grid are scaled to the higher productivity level, and the return rule measures computer-capital growth relative to a correspondingly scaled reference.[16]

The return channel raises the 2019 top-1% wealth share by 14.0 percentage points when dispersion remains linked to computer capital ($\psi = \psi^\star$, compared with $\psi = 0$; Table A.20 in Appendix D). Holding the return-premium distributions at their baseline forms, F_{19} and F_{67}, gives a contribution of 13.8 points. Both are close to the baseline contribution of +14.0 points. College attainment responds more strongly: with measured productivity and ICT-linked dispersion, the 2019 college share reaches 35%, compared with 29.8% in the baseline.

6.4 Alternative wealth series and shorter windows

The baseline calibration targets the 1967–2019 increase in the World Inequality Database. Two alternative series provide comparisons over shorter periods: Smith, Zidar, and Zwick (2023) report a 6.6-percentage-point rise in the top-1% wealth share over 1989–2016, and the Congressional Budget Office (2022) reports a 7.4-point rise over 1989–2019. I solve the additional 1989 and 2016 stationary equilibria using the baseline calibration. With the return channel active ($\psi = \psi^\star$), the model generates increases of 4.5 and 4.6 percentage points over the respective windows, equivalent to 68% and 62% of the observed changes (Table A.12 in Appendix D).

[15] With $\beta = 0.97$, the common return crosses zero near $\psi = 0.039$. With $\beta = 0.95$, it remains positive through $\psi = 0.085$, where $r = 0.31\%$; no stationary equilibrium was found at $\psi = 0.090$.

[16] Let $Z = 2.13$ denote productivity relative to 1967 and $s = Z^{1/(1-\alpha)} \approx 2.8$. I multiply the education cost, the asset grid, and K_c^{ref} in equation (9) by s. The education taste scale is multiplied by $s^{-0.5}$ to reflect the scaling of CRRA utility with risk aversion 1.5.

About one-third of the model's calibrated 1967–2019 increase occurs before 1989. Matching the larger increases in the alternative series over their shorter windows therefore requires a higher dispersion elasticity. The model's responses across tested values of ψ imply matching elasticities of approximately 0.055 for Smith, Zidar, and Zwick (2023) and 0.059 for the CBO series, a quarter to a third above the baseline value of 0.0441, with all other parameters unchanged (Table A.21 in Appendix D).[17]

6.5 The shape of the return distribution

The persistent return component estimated by Fagereng et al. (2020) is negatively skewed and has heavy tails, with skewness of −5.3 and kurtosis of 78. I replace the baseline Normal distribution with a two-component mixture constructed to match these moments and a standard deviation of 6.02 percentage points.[18]

Panel A of Table 8 recalibrates ϕ, κ, and b_{nc} to the same three 1967 labor-market targets while keeping return persistence at its baseline value. The mixture generates a 1967 top-1% wealth share of 43.0%, compared with 27.6% under the Normal distribution.[19] The local Pareto slope over the top 1–0.1% band is 0.86, compared with 1.35 in the baseline, indicating a thicker initial wealth tail.

With return dispersion fixed ($\psi = 0$), the top-1% share falls to 31.5% in 2019. At the baseline elasticity $\psi^\star$, widening dispersion raises the 2019 share by +9.9 percentage points relative to this fixed-dispersion economy. The resulting 2019 share is 41.39%, 1.58 points below its 1967 level. At $\psi = 0.060$, the historical change becomes positive, at 0.75 points. These comparisons start from the mixture's higher initial wealth concentration.

Panel B rescales the mixture to approximately match the baseline 1967 top-1% wealth share, keeping the household parameters and return persistence at their baseline values. Multiplying the return types by 0.70 reduces their standard deviation to 4.2 percentage points and gives an initial top-1% share of 27.6%.

With dispersion fixed ($\psi = 0$), the top-1% share falls to 19.0% in 2019, a decline of 8.6 percentage points. At the baseline elasticity $\psi^\star$, widening dispersion raises the 2019 share by +10.9 points,

[17] The estimate for the 1989–2016 window uses a short linear extrapolation, 0.0003 beyond the last solved 2016 point at $\psi = 0.055$.

[18] A gross-return floor and subsequent re-centering keep gross returns positive and the mean premium at zero. These adjustments change the moments of the implemented distribution.

[19] With all parameters held at their baseline values, the mixture gives a 1967 top-1% share of 44.3%.

Table 8: Return distribution and wealth concentration

Economy	Top-1% share (%)	Channel contribution (pp)	Change from 1967 (pp)
Panel A: Mixture with household parameters recalibrated			
1967	42.97	–	–
2019, fixed dispersion	31.47	–	−11.50
2019, $\psi = 0.030$	38.51	+7.04	−4.46
2019, $\psi = \psi^\star$	41.39	+9.92	−1.58
2019, $\psi = 0.060$	43.72	+12.25	+0.75
Panel B: Mixture scaled to match initial concentration			
1967	27.64	–	–
2019, fixed dispersion	19.00	–	−8.64
2019, $\psi = 0.030$	26.33	+7.32	−1.31
2019, $\psi = \psi^\star$	29.93	+10.93	+2.29
2019, $\psi = 0.060$	33.98	+14.98	+6.34

Note: Channel effects compare each panel's 2019 economy with its own fixed-dispersion economy ($\psi = 0$); historical changes use that panel's 1967 equilibrium. Differences use unrounded values; $\psi^\star = 0.0441$.
Panel A recalibrates ϕ, κ, and b_{nc} to the three labor-market targets, retaining baseline return persistence. Panel B retains baseline household parameters and persistence and scales mixture return types by 0.6984 to match initial top concentration approximately. Both panels apply a gross-return floor and re-center premia, changing the implemented distribution's moments.

compared with +14.0 in the baseline. The resulting 1967–2019 increase is +2.3 points. The channel's contribution is about one-fifth smaller under the mixture, which starts with lower return dispersion and experiences a smaller increase in it.[20]

At the higher elasticity $\psi = 0.060$, the channel contributes +15.0 percentage points, and the 1967–2019 increase reaches +6.3 points, within one point of the observed 7.2-point rise. Return shape and scale therefore matter for both initial wealth concentration and the magnitude of the channel. Widening dispersion has a large positive incremental effect in both mixture experiments. At the baseline elasticity, it reverses the historical decline when initial concentration is matched; with the higher initial concentration in Panel A, it offsets most of the decline.

7 Conclusion

Widening persistent return differences is the concentrating force in this model of computerization. Under the calibrated ICT-linked rule ($\psi = \psi^\star$), computer-capital accumulation widens these

[20] At $\psi^\star$, the standard deviation rises from 4.2 to 5.64 percentage points under the mixture, compared with 6.0 to 8.1 in the baseline. Per additional percentage point of return dispersion, the channel contributes about 7.6 points to the top-1% wealth share under the mixture and 6.8 under the Normal distribution.

differences enough for the measured ICT-price decline to raise the stationary top-1% wealth share by 6.5 percentage points, holding depreciation and education costs at their 2019 values. Holding premia at either their initial or baseline 2019 distribution, the same price decline instead lowers the share by 8.1–8.6 points. Higher wages and adjustments in the common return and financing tax spread wealth more broadly, even as employment shifts from routine toward abstract and manual tasks. The return channel more than offsets these equalizing responses.

At the 2019 benchmark inputs, widening dispersion raises the top-1% share by 13.98 percentage points relative to the economy retaining its initial dispersion ($\psi = 0$). This contribution offsets the decline under fixed dispersion and produces the calibrated 7.2-point increase between the 1967 and 2019 benchmarks. The production structure has substantial effects on the level of wealth concentration, task allocation, and college attainment, while the wealth effect of wider return dispersion remains large across different technologies and schooling restrictions. Its magnitude depends strongly on how long return advantages persist. Shortening expected return-type spells from 4.6 to 2.1 years reduces this contribution by about two-thirds. Sustained advantages allow high-return households to accumulate disproportionately, while their additional saving expands the capital stock and lowers the common return.

The quantitative magnitudes depend on the asset bound and the shape and scale of returns. The contribution of widening premia is larger at each higher asset bound tested, while the ICT-price effect at fixed premia remains negative. Under the alternative return distributions, widening continues to raise top shares relative to fixed dispersion; how much of the decline it offsets depends on initial concentration and return dispersion. These results point to the value of jointly disciplining the scale, shape, and persistence of household returns.

The empirical priority is to measure how these return characteristics change with technology. Such evidence would directly discipline the relationship calibrated here, while longitudinal wealth histories would help assess accumulation dynamics beyond the stationary comparisons (Hubmer et al., forthcoming). These questions also matter for artificial intelligence, whose task effects may differ from those of earlier computerization. AI could narrow wage differences while increasing wealth concentration (Rockall, Mendes Tavares, and Pizzinelli, 2025). The analysis directs attention beyond wages and employment to whether new technologies change who earns high returns and how long those advantages persist.

References

Andrews, Dan, Chiara Criscuolo, and Peter N. Gal. 2016. "The Best versus the Rest: The Global Productivity Slowdown, Divergence across Firms and the Role of Public Policy." OECD Productivity Working Papers No. 5. Paris: OECD Publishing.

Autor, David H., and David Dorn. 2013. "The Growth of Low-Skill Service Jobs and the Polarization of the US Labor Market." *American Economic Review* 103(5): 1553–1597.

Autor, David H., Frank Levy, and Richard J. Murnane. 2003. "The Skill Content of Recent Technological Change: An Empirical Exploration." *Quarterly Journal of Economics* 118(4): 1279–1333.

Bach, Laurent, Laurent E. Calvet, and Paolo Sodini. 2020. "Rich Pickings? Risk, Return, and Skill in Household Wealth." *American Economic Review* 110(9): 2703–2747.

Benhabib, Jess, Alberto Bisin, and Mi Luo. 2019. "Wealth Distribution and Social Mobility in the US: A Quantitative Approach." *American Economic Review* 109(5): 1623–1647.

Benhabib, Jess, Alberto Bisin, and Shenghao Zhu. 2011. "The Distribution of Wealth and Fiscal Policy in Economies with Finitely Lived Agents." *Econometrica* 79(1): 123–157.

Bessen, James. 2020. "Industry Concentration and Information Technology." *Journal of Law and Economics* 63(3): 531–555.

Blanchard, Olivier J. 1985. "Debt, Deficits, and Finite Horizons." *Journal of Political Economy* 93(2): 223–247.

Caines, Colin, Florian Hoffmann, and Gueorgui Kambourov. 2017. "Complex-Task Biased Technological Change and the Labor Market." *Review of Economic Dynamics* 25: 298–319.

Calligaris, Sara, Chiara Criscuolo, and Luca Marcolin. 2018. "Mark-ups in the Digital Era." OECD Science, Technology and Industry Working Papers 2018/10. Paris: OECD Publishing.

Congressional Budget Office. 2022. "Trends in the Distribution of Family Wealth, 1989 to 2019." Publication 57598. Washington, DC.

Cortes, Guido Matias, Nir Jaimovich, and Henry E. Siu. 2017. "Disappearing Routine Jobs: Who, How, and Why?" *Journal of Monetary Economics* 91: 69–87.

De Loecker, Jan, Jan Eeckhout, and Gabriel Unger. 2020. "The Rise of Market Power and the Macroeconomic Implications." *Quarterly Journal of Economics* 135(2): 561–644.

DiCecio, Riccardo. 2009. "Sticky Wages and Sectoral Labor Comovement." *Journal of Economic Dynamics and Control* 33(3): 538–553. https://doi.org/10.1016/j.jedc.2008.08.003.

Fagereng, Andreas, Luigi Guiso, Davide Malacrino, and Luigi Pistaferri. 2020. "Heterogeneity and Persistence in Returns to Wealth." *Econometrica* 88(1): 115–170.

Flood, Sarah, Miriam King, Renae Rodgers, Steven Ruggles, J. Robert Warren, Daniel Backman, Etienne Breton, Grace Cooper, Julia A. Rivera Drew, Stephanie Richards, David Van Riper, and Kari C. W. Williams. 2025. *IPUMS CPS: Version 13.0* [dataset]. Minneapolis, MN: IPUMS. https://doi.org/10.18128/D030.V13.0.

Furman, Jason, and Peter Orszag. 2015. "A Firm-Level Perspective on the Role of Rents in the Rise in Inequality." Presentation at "A Just Society," a centennial event in honor of Joseph Stiglitz, Columbia University, October 16.

Gabaix, Xavier, Jean-Michel Lasry, Pierre-Louis Lions, and Benjamin Moll. 2016. "The Dynamics of Inequality." *Econometrica* 84(6): 2071–2111.

Gârleanu, Nicolae, Leonid Kogan, and Stavros Panageas. 2012. "Displacement Risk and Asset Returns." *Journal of Financial Economics* 105(3): 491–510.

Gomez, Matthieu, and Émilien Gouin-Bonenfant. 2024. "Wealth Inequality in a Low Rate Environment." *Econometrica* 92(1): 201–246.

Goos, Maarten, Alan Manning, and Anna Salomons. 2014. "Explaining Job Polarization: Routine-Biased Technological Change and Offshoring." *American Economic Review* 104(8): 2509–2526.

Hubmer, Joachim, Elin Halvorsen, Sergio Salgado, and Serdar Ozkan. Forthcoming. "Why Are the Wealthiest So Wealthy? New Longitudinal Empirical Evidence and Implications for Theories of Wealth Inequality." *Econometrica*.

Hubmer, Joachim, Per Krusell, and Anthony A. Smith Jr. 2021. "Sources of US Wealth Inequality: Past, Present, and Future." *NBER Macroeconomics Annual* 35: 391–455.

Jaimovich, Nir, and Henry E. Siu. 2020. "Job Polarization and Jobless Recoveries." *Review of Economics and Statistics* 102(1): 129–147.

Kacperczyk, Marcin, Jaromir Nosal, and Luminita Stevens. 2019. "Investor Sophistication and Capital Income Inequality." *Journal of Monetary Economics* 107: 18–31.

Kogan, Leonid, Dimitris Papanikolaou, and Noah Stoffman. 2020. "Left Behind: Creative Destruction, Inequality, and the Stock Market." *Journal of Political Economy* 128(3): 855–906.

Koru, Ömer Faruk. 2024. "Automation and Top Wealth Inequality." Working paper, Pennsylvania State University, October 2024. https://omerfarukkoru.com/Papers/automation_top_wealth.pdf.

Krusell, Per, Lee E. Ohanian, José-Víctor Ríos-Rull, and Giovanni L. Violante. 2000. "Capital-Skill Complementarity and Inequality: A Macroeconomic Analysis." *Econometrica* 68(5): 1029–1053.

Lashkari, Danial, Arthur Bauer, and Jocelyn Boussard. 2024. "Information Technology and Returns to Scale." *American Economic Review* 114(6): 1769–1815.

Moll, Benjamin, Lukasz Rachel, and Pascual Restrepo. 2022. "Uneven Growth: Automation's Impact on Income and Wealth Inequality." *Econometrica* 90(6): 2645–2683.

Muto, Ichiro, Fumitaka Nakamura, and Makoto Nirei. 2024. "Digitalization, Entrepreneurship, and Wealth Inequality." IMES Discussion Paper 2024-E-1, Bank of Japan.

Ohanian, Lee E., Musa Orak, and Shihan Shen. 2023. "Revisiting Capital-Skill Complementarity, Inequality, and Labor Share." *Review of Economic Dynamics* 51: 479–505.

Orak, Musa. 2016. "Essays on the Impact of Technological Progress on the U.S. Labor Markets." Ph.D. dissertation, University of California, Los Angeles. eScholarship: https://escholarship.org/uc/item/0m97r8pz. Chapter 3, "Job Polarization, Skill Accumulation and Wealth Inequality."

Orak, Musa. 2017. "Capital-Task Complementarity and the Decline of the U.S. Labor Share of Income." International Finance Discussion Papers 1200, Board of Governors of the Federal Reserve System, March.

Prettner, Klaus, and Holger Strulik. 2020. "Innovation, Automation, and Inequality: Policy Challenges in the Race against the Machine." *Journal of Monetary Economics* 116: 249–265.

Rockall, Emma J., Marina Mendes Tavares, and Carlo Pizzinelli. 2025. "AI Adoption and Inequality." IMF Working Paper 25/68.

Saez, Emmanuel, and Gabriel Zucman. 2016. "Wealth Inequality in the United States since 1913: Evidence from Capitalized Income Tax Data." *Quarterly Journal of Economics* 131(2): 519–578.

Smith, Matthew, Owen Zidar, and Eric Zwick. 2023. "Top Wealth in America: New Estimates under Heterogeneous Returns." *Quarterly Journal of Economics* 138(1): 515–573.

Stachurski, John, and Alexis Akira Toda. 2019. "An Impossibility Theorem for Wealth in Heterogeneous-Agent Models with Limited Heterogeneity." *Journal of Economic Theory* 182: 1–24.

vom Lehn, Christian. 2020. "Labor Market Polarization, the Decline of Routine Work, and Technological Change: A Quantitative Analysis." *Journal of Monetary Economics* 110: 62–80.

Wolff, Edward N. 2021. "Household Wealth Trends in the United States, 1962 to 2019: Median Wealth Rebounds... But Not Enough." NBER Working Paper 28383.

World Inequality Database. 2022. "United States: Net Personal Wealth, Top 1% and Top 10% Shares." https://wid.world (accessed 2022).

Appendix

A GMM estimation of the production block

This appendix gives the moment conditions and estimation checks for Section 3.2. The production function is

$$Y = ZK_s^{\alpha} M^{\gamma} L_m^{1-\alpha-\gamma}, \qquad M = \left[\mu L_r^{\sigma} + (1-\mu)G^{\sigma}\right]^{1/\sigma}, \qquad G = \left[\xi L_a^{\lambda} + (1-\xi)K_c^{\lambda}\right]^{1/\lambda}.$$

Labor inputs are measured in efficiency units. The historical no-arbitrage condition equates the one-year returns on structural and ICT capital, including the change in the relative ICT price p_c. Capital marginal products are evaluated using observed output; a separate parameterization of neutral productivity is therefore unnecessary for estimation.

Moment conditions. Let $\text{MPK}_s = \alpha Y/K_s$ and $\text{MPK}_c = \partial Y/\partial K_c$. The four residuals are

$$\begin{aligned}
g_1 &= \text{MPK}_{s,t+1} + (1-\delta_{s,t+1}) - (1-\delta_{c,t+1})\tfrac{p_{c,t+1}}{p_{c,t}} - \tfrac{1}{p_{c,t}}\text{MPK}_{c,t+1} && \text{(capital no-arbitrage)},\\
g_2 &= (1-\alpha-\gamma) + \tfrac{\gamma}{M^{\sigma}}\left[\mu L_r^{\sigma} + (1-\mu)\xi L_a^{\lambda} G^{\sigma-\lambda}\right] - s_t^L && \text{(aggregate labor share)},\\
g_3 &= \tfrac{1-\mu}{\mu}\,\xi\, L_a^{\lambda}\, G^{\sigma-\lambda}\, L_r^{-\sigma} - \tfrac{w_a L_a}{w_r L_r} && \text{(abstract/routine wage bill)},\\
g_4 &= (1-\alpha-\gamma)\,\tfrac{M^{\sigma}}{\gamma\mu L_r^{\sigma}} - \tfrac{w_m L_m}{w_r L_r} && \text{(manual/routine wage bill)}.
\end{aligned}$$

The manual-to-routine wage-bill condition g_4 supplements the conditions used by Ohanian, Orak, and Shen (2023) and helps identify the manual share. The baseline specification interacts each residual with $q_t = (1, K_{c,t}, K_{s,t}, p_{c,t})$, giving 16 moments for six parameters. Two-step GMM uses a Newey–West HAC weighting matrix with a Bartlett kernel and three lags. Data cover 1967–2019. Since g_1 contains one-year-ahead terms, the common moment sample is 1967–2018 ($n = 52$).

The robustness specifications vary the weighting matrix and instrument set. The largest set is

$$q_t^{+} = (K_{c,t}, K_{s,t}, K_{c,t-1}, K_{s,t-1}, p_{c,t-1}, \text{year}_t, \text{oecd}_{t-1}),$$

where oecd_t is the OECD composite leading indicator. This gives 28 moments and 22 overidentifying

restrictions. Intermediate specifications remove the trend and OECD instrument or use only the constant and contemporaneous capital stocks.

Estimates and fit. The estimated elasticities are $1/(1-\sigma) = 3.29$ and $1/(1-\lambda) = 0.94$. The first indicates substantial substitution between routine labor and the abstract–ICT bundle; the second is close to unity. The baseline Hansen statistic is $J = 10.9$ with 10 degrees of freedom ($p = 0.36$).

Table A.1 reports estimates under alternative instrument sets and weighting matrices. The routine–bundle elasticity ranges from 3.24 to 3.52, and the abstract–ICT elasticity from 0.94 to 0.96. The unadjusted weighting matrix gives $J = 111.4$ ($p < 0.001$); accounting for serial correlation changes the test statistic substantially while leaving the elasticities similar. The baseline uses four instruments to limit the dimension of the estimated weighting matrix relative to the 52 annual observations. The three-instrument specification gives similar elasticities and $p = 0.11$.

Neutral productivity. After estimating the production parameters, I recover the productivity residual as

$$Z_t = \frac{Y_t^{\text{obs}}}{K_{s,t}^{\alpha} M_t^{\gamma} L_{m,t}^{1-\alpha-\gamma}}.$$

Using the same output and input series as in estimation gives $Z_{2019}/Z_{1967} = 2.13$. The baseline holds productivity at its 1967 level; Section 6 uses this measured increase in the neutral-productivity counterfactual.

Table A.1: Elasticities under alternative weighting matrices and instruments

Specification	Weight	Instr.	$\frac{1}{1-\sigma}$	$\frac{1}{1-\lambda}$	J	df	p
Unadjusted weighting	unadjusted	7	3.52	0.96	111.4	22	< 0.001
Full instruments	HAC	7	3.27	0.94	13.3	22	0.92
Drop trend, OECD	HAC	5	3.24	0.94	12.7	14	0.55
Levels $\{1, K_c, K_s, p_c\}$ (baseline)	HAC	4	3.29	0.94	10.9	10	0.36
Minimal $\{1, K_c, K_s\}$	HAC	3	3.30	0.94	10.4	6	0.11

Note: Each row re-estimates all six production parameters. HAC uses a Newey–West estimate of the long-run covariance matrix with a Bartlett kernel and three lags. Each instrument interacts with all four residuals, so the number of moments is four times the instrument count and the number of overidentifying restrictions is six fewer. All specifications use the same moment sample. The baseline is the four-instrument levels specification.

B Recursive formulation of the household problem

This appendix states the recursive household problem underlying equations (5)–(9). The individual state is (a, h, η, ω, z): assets a, education status $h \in \{U, S\}$ (non-college or college), the lifetime routine-efficiency type η, the persistent return type ω, and idiosyncratic productivity z. Flow utility $u(c)$ is CRRA with a coefficient of relative risk aversion of 1.5 and requires $c > 0$; the discount factor is β, the per-period death probability p_{die}, and the return-type refresh probability p_{ref}. Productivity follows the Markov kernel $\Pi(z' \mid z)$; newborn routine-efficiency and return types are drawn from the distributions F_η and F_ω.

Prices and income. At a benchmark with computer capital K_c, the return channel (9) maps each return type into a premium

$$\hat{\omega} \;=\; \omega \left(K_c / K_c^{\text{ref}}\right)^{\psi}, \qquad K_c^{\text{ref}} = K_c^{1967},$$

so that the gross return on positive net worth is $1 + r + \hat{\omega}$ and on debt $1 + r$. Labor income depends on education. A college household supplies abstract labor at efficiency κ and earns $y_S(z) = w_a \kappa z$. A non-college household of type η earns $y_U(\eta, z)$ from the three-way comparative-advantage sort of (5). Both face the common lump-sum tax τ that finances the aggregate return premium.

Continuation value. Let $g_h(a, \eta, \omega, z)$ be the optimal asset policy. After a household chooses next-period assets a', three things can happen before the next decision. With probability p_{die} it dies and is replaced by a newborn who inherits (a', z') but draws fresh routine-efficiency and return types and re-chooses education, delivering the newborn value v_0 integrated over (η', ω'). With probability $(1 - p_{\text{die}})p_{\text{ref}}$ it survives but its return type is refreshed to a fresh draw ω', keeping h and η. With the remaining probability it survives with both types unchanged. Collecting these and taking the expectation over z', the post-decision continuation for an h-household is

$$\begin{aligned} W_h(a', \eta, \omega, z) \;=\; \mathbb{E}_{z'|z}\Big[& (1 - p_{\text{die}})(1 - p_{\text{ref}})\, v_h(a', \eta, \omega, z') \\ & + (1 - p_{\text{die}})\, p_{\text{ref}} \int v_h(a', \eta, \omega', z')\, dF_\omega(\omega') \\ & + p_{\text{die}} \iint v_0(a', \eta', \omega', z')\, dF_\eta(\eta')\, dF_\omega(\omega') \Big]. \end{aligned} \tag{11}$$

For college households the value v_S does not depend on η, so the first two terms drop the η argument; the newborn term is unchanged because a newborn redraws η' regardless.

Bellman equations. Given prices, the non-college and college value functions solve

$$v_U(a,\eta,\omega,z) = \max_{\underline{a}\le a'\le \bar{a}} u\big((1+r+\hat{\omega}\,\mathbf{1}\{a\ge 0\})\,a + y_U(\eta,z) - \tau - a'\big) + \beta\, W_U(a',\eta,\omega,z), \tag{12}$$

$$v_S(a,\omega,z) = \max_{\underline{a}\le a'\le \bar{a}} u\big((1+r+\hat{\omega}\,\mathbf{1}\{a\ge 0\})\,a + y_S(z) - \tau - a'\big) + \beta\, W_S(a',\omega,z). \tag{13}$$

Routine efficiency remains fixed during a household's life, while its return type can change. The continuation value accounts for both return-type refresh during survival and the newborn's choices after inheritance.

Newborn education choice. A newborn inheriting (a',z') with fresh types (η',ω') compares entering as non-college against paying the schooling cost ϕ and entering as college, as in (6). With a scale-ϑ extreme-value taste shock and the affordability requirement $a'-\phi\ge\underline{a}$, the newborn value is the inclusive value of the two options,

$$v_0(a',\eta',\omega',z') = \begin{cases} \vartheta\,\log\Big[\exp\big(v_U(a',\eta',\omega',z')/\vartheta\big) + \exp\big(v_S(a'-\phi,\omega',z')/\vartheta\big)\Big], & a'-\phi\ge\underline{a}, \\ v_U(a',\eta',\omega',z'), & a'-\phi<\underline{a}, \end{cases} \tag{14}$$

and the associated college-entry probability is the logit (7), evaluated at post-tuition assets $a'-\phi$ inside v_S. Newborns with inherited assets below the tuition threshold enter as non-college households.

Stationary distribution. Let ν be a probability measure over the state space (a,h,η,ω,z) and let $\mathcal{T}$ be the operator that pushes ν one period forward under the asset policies g_h, the productivity kernel Π, the death/refresh transitions of the household types, and the newborn education rule (14). A stationary equilibrium at given benchmark inputs is a fixed point $\nu=\mathcal{T}\nu$ together with value and policy functions solving (12)–(14), factor prices equal to marginal products, the two no-arbitrage conditions (4) determining the capital split and the common return, capital-market

clearing $A = K_s + p_c K_c = \int a \, dv$, efficiency-unit labor supplies (L_a, L_r, L_m) aggregated from the household sort, and the tax τ balancing the return-premium budget of Section 2.2.

C Computation

I solve jointly for equilibrium prices and the stationary household distribution. Prices determine household choices, which in turn determine aggregate capital and labor supplies. The algorithm iterates between these calculations until markets clear and the household distribution is stationary.

State space. The baseline asset grid has 300 points between 0 and 2,000, with more points near zero. Routine efficiency η is represented by 12 equally weighted points from its lognormal distribution, the return type ω by 9 weighted points, and productivity z by its two states. Education status distinguishes college and non-college households.

Equilibrium algorithm. For each benchmark, I begin with guesses for aggregate wealth A, labor supplies (L_a, L_r, L_m), and the financing tax τ, and repeat the following steps:

1. *Compute prices and returns.* Allocate wealth between structural and computer capital using the capital-market and no-arbitrage conditions, equations (3) and (4). Calculate wages and the common return from marginal products. Set return premia using the ICT-linked rule or the premium distribution specified for the counterfactual.

2. *Solve household choices.* At these prices and tax, solve the household problem in Appendix B for saving, occupation, and newborn college entry. Repeatedly update lifetime values and choices until the values converge.

3. *Find the stationary distribution.* Apply these choices, productivity shocks, return-type refresh, and death and inheritance to the household population. Repeat this update until the distribution converges.

4. *Update the aggregate guesses.* Aggregate household wealth, labor supplies, and the premium bill. Move the guesses partway toward these totals and repeat until the market-clearing gaps satisfy the convergence criteria.

Choices between grid points. Saving is continuous: I search between neighboring asset-grid points and interpolate future values. When updating the distribution, I divide each household's mass between the two neighboring asset points with weights that preserve its chosen saving. Likewise, an efficiency bin containing an occupational cutoff is divided across tasks using the lognormal distribution. An asset cell containing the tuition threshold is divided according to affordability. This treatment keeps employment and college entry from jumping as prices or tuition change.

Reporting and accuracy. I average the aggregate allocation over the final 24 equilibrium iterations, calculate prices at that allocation, and solve the household problem and distribution again. Statistics labeled *window means* are averaged over those 24 iterations; *single evaluations* are computed once at the reported allocation and prices. I check market clearing, agreement between the two sets of wealth shares, and stability over the final iterations. Value and distribution updates use tolerances of 10^{-7} and 10^{-10}, respectively; the population mass at the upper asset point must be below 10^{-4}.

Calibration. Each trial parameter vector requires a full equilibrium calculation. I adjust ϕ, κ, and b_{nc} to match the three 1967 labor-market targets, and the return-type refresh probability to match the 1967 top-1% wealth share. I repeat these adjustments until all four moments are within 0.1 percentage points of their targets. With the initial economy calibrated, I adjust ψ to match the 1967–2019 increase in the top-1% share.

The upper asset bound. I assess numerical sensitivity by increasing the numbers of asset and return-type points and by raising the upper asset bound (Tables 7 and A.18). The bound matters because very wealthy households can hold substantial aggregate wealth even when they are few in number. Tables A.19 and A.11 describe the resulting upper tails. The reported equilibria use a bounded asset space.

Financing feasibility. A household with zero wealth must be able to consume after paying the lump-sum tax. For the lowest-income household, this requires $w_m z_\ell - \tau > 0$. I monitor this margin while varying dispersion and persistence, using each solution to initialize the next calculation. The last solved baseline dispersion case has $\psi = 0.075$ and a margin of 0.014; the attempt at 0.080

leaves the feasible region. With wider premia, the last solved return-type duration is 6.23 years, with a margin of 0.029; the 7.28-year case does not converge to an equilibrium. At $\beta = 0.95$, the corresponding elasticity values are 0.085 (margin 0.019) and 0.090. These unsuccessful calculations leave equilibrium existence beyond the reported cases unresolved. Under proportional financing, zero-wealth households pay no premium levy.

D Additional results

D.1 Parameters and calibration

Table A.2 reports all parameter values and their sources or targets. Table A.3 compares the baseline, which targets the 1967 top-1% share, with the alternative calibration that targets a local Pareto slope of 1.50.

Table A.2: Parameters

Parameter	Value	Source / target
Preferences and demographics (externally set)		
Risk aversion	1.5	standard
Discount factor β	0.96	standard
Death probability p_{die}	0.0222	45-year working life
Productivity z, persistence	$\{0.4, 1.0\}$, 0.8	standard
Production (GMM-estimated, Section 3.2)		
Structural-capital share α	0.267	GMM
Non-manual composite share γ	0.692	GMM
Manual share $1 - \alpha - \gamma$	0.041	GMM
Routine CES weight μ	0.339	GMM
Abstract CES weight ξ	0.904	GMM
Routine–abstract/ICT-bundle elasticity $1/(1-\sigma)$	3.29	GMM ($\sigma = 0.696$)
Abstract–ICT elasticity $1/(1-\lambda)$	0.94	GMM ($\lambda = -0.068$)
Structural depreciation δ_s	0.05	standard
ICT depreciation δ_c: 1967 $\rightarrow$ 2019	0.142 $\rightarrow$ 0.179	measured
p_c: 1967 $\rightarrow$ 2019	$\times 1/385$	measured ICT relative price
Household, calibrated to the 1967 cross-section (Table 2)		
College efficiency κ	1.49	abstract share of abstract-plus-routine labor, $L_a/(L_a + L_r)$
Education cost ϕ	1.80	college share of the employed
Non-college abstract scale b_{nc}	0.78	abstract-task employment share
Abstract-efficiency curvature ρ	1.5	fixed
Routine-efficiency dispersion σ_η	0.20	fixed
Education taste ϑ	0.02	set; sensitivity in Section 3.3
1967 return SD	6.0 pp	Fagereng et al. (2020) (6.02 pp)
Refresh rate p_{ref}	0.198	1967 top-1% wealth share (27.66%, WID); spells of 4.64 years
Chosen with post-1967 outcomes in view		
Dispersion elasticity ψ	0.0441	1967–2019 WID rise in the top-1% share
Education-cost pass-through χ	0.30	later path of college attainment

Note: The firm block is estimated by GMM; the household parameters are calibrated jointly to the targets in Table 2. Values are rounded.

Table A.3: Calibrating return persistence: slope target and level target

	Slope-targeted (comparison)	Level-targeted (baseline)
Persistence calibration		
Target of p_{ref}	slope 1.50	top-1% share 27.66%
Refresh rate p_{ref}	0.236	0.198
Expected return-type duration (years)	3.96	4.64
1967 local Pareto slope, top 1–0.1%	1.50†	1.35
1967 top-1% share (%)	22.90	27.64†
Dispersion elasticity $\psi^{\star}$	0.0458	0.0441
1967–2019 rise in the top-1% share (pp)	+7.20†	+7.20†
2019 equilibria at the benchmark inputs		
Top-1% share, fixed dispersion (%)	16.65	20.86
Top-1% share, wider dispersion (%)	30.10	34.84
Fixed-dispersion change, 1967–2019 (pp)	−6.25	−6.78
Return-channel contribution (pp)	+13.45	+13.98
Common return r, wider dispersion (%)	1.23	0.86
ICT-price effects on the top-1% share (pp)		
1967 premium distribution, $B - A$	−7.57	−8.14
2019 premium distribution, $D - C$	−8.51	−8.61
ICT-linked rule, $D_L - E$	+6.50	+6.50

Note: †Calibration target. The baseline targets the 1967 WID top-1% share (27.66%); the alternative imposes a local Pareto slope of 1.50 over the top 1–0.1% band. In both, ϕ, κ, and b_{nc} match the three labor-market targets, initial return dispersion is 6.0 percentage points, and ψ matches the WID increase of 7.19 points using the calibration's own 1967 ICT-capital reference. Shares are window means at the 2,000 asset bound.
ICT-price comparisons hold tuition and depreciation at 2019 values. A, B use F_{67}; C, D use F_{19}; E, D_L use the ICT-linked rule ($\psi = \psi^{\star}$), all within the corresponding calibration.

D.2 Computerization experiments

Table A.4 reports the equilibria used in Section 4.1. Economies A and B hold return premia at F_{67}, and C and D at F_{19}; within each pair, the ICT price falls from its 1967 to its 2019 value. Economies E and D_L apply the ICT-linked rule ($\psi = \psi^\star$) at the old and new prices. All use 2019 tuition and ICT depreciation. The wider-bound comparisons in Table A.6 use the same definitions.

Table A.5 holds tuition and depreciation at their 1967 values. With initial premia, the ICT-price decline lowers the top-1% share from 27.64% to 19.85%; with wider premia, it lowers the share from 42.17% to 33.67%. Thus, the equalizing price effect also appears when tuition and ICT depreciation remain at their initial values.

Table A.4: Computerization experiments: 2019 tuition and depreciation

	A 1967 price F_{67}	B 2019 price F_{67}	C 1967 price F_{19}	D 2019 price F_{19}	E 1967 price linked	D_L 2019 price linked
ICT price p_c	246	0.639	246	0.639	246	0.639
Tuition ϕ	2.097	2.097	2.097	2.097	2.097	2.097
ICT depreciation δ_c	0.179	0.179	0.179	0.179	0.179	0.179
Premium SD (pp)	6.00	6.00	8.06	8.06	5.92	8.06
Top-1% share (%)	29.00	20.86	43.45	34.84	28.34	34.84
Top-10% share (%)	56.76	48.52	67.72	60.76	56.24	60.76
Gini	0.683	0.630	0.765	0.720	0.679	0.720
Bottom-50% share (%)	9.04	9.89	6.40	7.18	9.17	7.18
Mean wealth	1.215	2.473	1.490	2.949	1.207	2.949
Median wealth	0.495	1.175	0.444	1.017	0.498	1.017
Common return r (%)	2.06	1.76	1.10	0.86	2.09	0.86
Total return $\bar{r}_W$ (%)	3.47	3.11	3.56	3.23	3.47	3.23
Wage w_a	0.326	0.529	0.346	0.564	0.326	0.564
Wage w_r	0.278	0.428	0.295	0.451	0.278	0.451
Wage w_m	0.211	0.345	0.224	0.361	0.211	0.361
Output Y	0.305	0.586	0.325	0.609	0.305	0.609
ICT capital K_c	0.000252	0.255	0.000285	0.276	0.000251	0.276
College attainment (%)	7.96	32.55	8.48	29.78	7.96	29.78
Abstract-task employment (%)	24.82	58.57	25.35	58.72	24.80	58.72
of which non-college (%)	16.86	26.02	16.87	28.95	16.84	28.95
Routine-task employment (%)	66.64	31.37	66.08	31.28	66.66	31.28
Manual-task employment (%)	8.54	10.06	8.57	10.00	8.54	10.00
Premium tax τ	0.0172	0.0333	0.0365	0.0700	0.0167	0.0700

Note: All economies use 2019 tuition and depreciation and the baseline calibration and asset bound. F_{67} retains initial return dispersion ($\psi = 0$); F_{19} fixes the premium distribution generated by the baseline 2019 economy. Linked economies apply equation (9) at $\psi = \psi^\star$; D and D_L agree at the displayed precision. Total return $\bar{r}_W$ is wealth-weighted, net of depreciation, and before the financing tax. Wages are per efficiency unit. Top shares, the Gini, and college attainment are window means; other distributional statistics use the evaluated stationary distribution. Prices and capital stocks refer to the reported allocation.

Table A.5: Computerization experiments: 1967 tuition and depreciation

	A_0 1967 price F_{67}	B_0 2019 price F_{67}	C_0 1967 price F_{19}	D_0 2019 price F_{19}
ICT price p_c	246	0.639	246	0.639
Tuition ϕ	1.797	1.797	1.797	1.797
ICT depreciation δ_c	0.142	0.142	0.142	0.142
Premium SD (pp)	6.00	6.00	8.06	8.06
Top-1% share (%)	27.64	19.85	42.17	33.67
Top-10% share (%)	55.57	46.18	66.73	58.92
Gini	0.679	0.599	0.761	0.699
Bottom-50% share (%)	8.97	11.82	6.41	8.24
Mean wealth	1.312	2.745	1.601	3.261
Median wealth	0.532	1.588	0.478	1.321
Common return r (%)	2.01	1.75	1.06	0.85
Total return $\bar{r}_W$ (%)	3.41	3.08	3.50	3.19
Wage w_a	0.328	0.533	0.349	0.570
Wage w_r	0.284	0.444	0.301	0.466
Wage w_m	0.218	0.369	0.231	0.383
Output Y	0.322	0.639	0.342	0.662
ICT capital K_c	0.000344	0.347	0.000391	0.377
College attainment (%)	13.10	44.01	12.88	39.89
Abstract-task employment (%)	26.21	60.86	26.77	60.46
of which non-college (%)	13.10	16.85	13.88	20.57
Routine-task employment (%)	65.04	28.87	64.47	29.29
Manual-task employment (%)	8.76	10.27	8.76	10.24
Premium tax τ	0.0185	0.0363	0.0391	0.0764

Note: Tuition and ICT depreciation are held at their 1967 values; A_0 is the 1967 equilibrium. Premium distributions, calibration, asset bound, and reporting conventions follow Table A.4. Total return $\bar{r}_W$ is wealth-weighted, net of depreciation, and before the financing tax.

Table A.6: Matched asset-bound comparison of the computerization effects

Top-1% share (pp)	$\bar{a}$ = 2,000	$\bar{a}$ = 4,000	Difference
Panel A. Level-targeted calibration			
ICT-price effect, initial premia ($B - A$)	−8.14	−8.63	−0.49
ICT-price effect, 2019 premia ($D - C$)	−8.61	−8.71	−0.10
Wider premia, 1967 ICT price ($C - A$)	+14.45	+15.69	+1.24
Wider premia, 2019 ICT price ($D - B$)	+13.98	+15.60	+1.63
Interaction	−0.47	−0.09	+0.38
Linked rule: ICT-price effect ($D_L - E$)	+6.50	+7.70	+1.20
premium adjustment at 1967 price ($C - E$)	+15.11	+16.40	+1.30
Panel B. Slope-targeted calibration			
ICT-price effect, initial premia ($B - A$)	−7.57	−8.06	−0.49
ICT-price effect, 2019 premia ($D - C$)	−8.51	−8.77	−0.27
Wider premia, 1967 ICT price ($C - A$)	+14.39	+15.65	+1.26
Wider premia, 2019 ICT price ($D - B$)	+13.45	+14.93	+1.48
Interaction	−0.94	−0.72	+0.22
Linked rule: ICT-price effect ($D_L - E$)	+6.50	+7.54	+1.05
premium adjustment at 1967 price ($C - E$)	+15.00	+16.32	+1.31

Note: Entries are differences in top-1% wealth shares, in percentage points, within each asset bound; the last column shows how each contrast changes when the bound doubles. All economies use 2019 tuition and depreciation. A, B fix premia at F_{67} and C, D at F_{19}; E, D_L apply the ICT-linked rule at their own computer capital ($\psi = \psi^{\star}$). Each panel uses its calibration's premium distributions and rule. The interaction is $(D - B) - (C - A)$, the change in the widening effect when the ICT price falls. Shares are window means.

Tables A.7 and A.8 report the partial-equilibrium decomposition for additional statistics. For a statistic S, let S_{ij} use wages from the old-price ($i = 0$) or new-price ($i = 1$) economy and the common return and tax from the old-price ($j = 0$) or new-price ($j = 1$) economy. The contributions averaged over the two orders are

$$\Delta_W = \tfrac{1}{2}\big[(S_{10} - S_{00}) + (S_{11} - S_{01})\big], \qquad \Delta_R = \tfrac{1}{2}\big[(S_{01} - S_{00}) + (S_{11} - S_{10})\big].$$

They sum to $S_{11} - S_{00}$. The interaction is $S_{11} - S_{10} - S_{01} + S_{00}$. Premium distributions and tuition remain fixed within each calculation; households and the stationary distribution respond to the specified prices. Hybrid combinations impose prices and the tax independently of market clearing and premium-budget balance.

Table A.7: ICT-price decomposition at F_{67}

Panel A: Levels and total changes

Statistic	S_{00}	S_{10}	S_{01}	S_{11}	Total
Top 1%	29.00	26.47	22.51	20.86	−8.14
Top 10%	56.76	53.25	51.22	48.52	−8.24
Top 0.1%	16.03	13.19	11.36	9.90	−6.13
Gini	68.33	66.03	63.82	63.05	−5.28
College	7.96	37.85	6.59	32.55	+24.59
Mean wealth	1.215	3.241	0.985	2.473	+1.257
Median wealth	0.495	1.472	0.468	1.175	+0.680
Bottom 50%	9.04	9.20	10.72	9.89	+0.85

Panel B: Contributions in each order and their averages

	Wages first		Return/tax first		Order averages		
Statistic	W	R	R	W	W	R	Interaction
Top 1%	−2.53	−5.61	−6.49	−1.65	−2.09	−6.05	+0.89
Top 10%	−3.51	−4.73	−5.54	−2.70	−3.11	−5.14	+0.81
Top 0.1%	−2.85	−3.29	−4.67	−1.46	−2.15	−3.98	+1.39
Gini	−2.30	−2.98	−4.51	−0.77	−1.54	−3.75	+1.53
College	+29.88	−5.30	−1.37	+25.96	+27.92	−3.33	−3.92
Mean wealth	+2.026	−0.768	−0.230	+1.488	+1.757	−0.499	−0.538
Median wealth	+0.977	−0.297	−0.027	+0.706	+0.842	−0.162	−0.271
Bottom 50%	+0.16	+0.69	+1.68	−0.84	−0.34	+1.18	−1.00

Note: S_{ij} uses old-price (0) or new-price (1) task wages (i) and common return and tax (j). W denotes wages and R the return and tax. Premia and tuition remain fixed; households and the stationary distribution respond at the imposed prices and tax, independently of market clearing and premium-budget balance. Shares and college attainment are percentages; the Gini is multiplied by 100. Changes in these statistics are percentage points. Wealth is in model units. Shares are single evaluations at the stated prices (Appendix C); differences use unrounded values. The interaction is $S_{11} - S_{10} - S_{01} + S_{00}$.

Table A.8: ICT-price decomposition at F_{19}

Panel A: Levels and total changes

Statistic	S_{00}	S_{10}	S_{01}	S_{11}	Total
Top 1%	43.44	38.48	39.62	34.84	−8.61
Top 10%	67.72	63.96	64.28	60.76	−6.96
Top 0.1%	26.67	20.51	23.67	18.70	−7.98
Gini	76.53	74.52	73.36	72.04	−4.49
College	8.48	30.66	9.64	29.78	+21.30
Mean wealth	1.490	3.285	1.563	2.949	+1.459
Median wealth	0.444	1.026	0.527	1.017	+0.573
Bottom 50%	6.40	6.27	7.82	7.18	+0.79

Panel B: Contributions in each order and their averages

	Wages first		Return/tax first		Order averages		
Statistic	W	R	R	W	W	R	Interaction
Top 1%	−4.96	−3.64	−3.83	−4.78	−4.87	−3.74	+0.18
Top 10%	−3.77	−3.19	−3.44	−3.52	−3.64	−3.32	+0.25
Top 0.1%	−6.16	−1.82	−3.01	−4.97	−5.56	−2.41	+1.19
Gini	−2.01	−2.48	−3.17	−1.32	−1.66	−2.83	+0.69
College	+22.18	−0.88	+1.16	+20.14	+21.16	+0.14	−2.04
Mean wealth	+1.795	−0.336	+0.073	+1.385	+1.590	−0.132	−0.410
Median wealth	+0.582	−0.009	+0.083	+0.490	+0.536	+0.037	−0.093
Bottom 50%	−0.12	+0.91	+1.42	−0.64	−0.38	+1.17	−0.52

Note: S_{ij} uses old-price (0) or new-price (1) task wages (i) and common return and tax (j). W denotes wages and R the return and tax. Premia and tuition remain fixed; households and the stationary distribution respond at the imposed prices and tax, independently of market clearing and premium-budget balance. Shares and college attainment are percentages; the Gini is multiplied by 100. Changes in these statistics are percentage points. Wealth is in model units. Shares are single evaluations at the stated prices (Appendix C); differences use unrounded values. The interaction is $S_{11} - S_{10} - S_{01} + S_{00}$.

D.3 Historical benchmark comparisons

Table A.9 compares wealth shares and common and total returns at the four benchmarks with widening dispersion ($\psi = \psi^\star$) and fixed dispersion ($\psi = 0$). Table A.10 decomposes the historical fixed-dispersion decline, allowing both wages and tuition to change. Starting from 1967, the 2019 wages and education cost lower the top-1% share by 2.30 percentage points, while the 2019 common return and tax lower it by 5.12 points. Together they lower the share by 6.78 points, with an interaction of 0.64 points.[21] This comparison includes the historical changes in tuition and ICT depreciation; the price experiment in Section 4.1 holds these inputs at their 2019 values.

Table A.9: Top wealth shares and household returns at the benchmark years

	1967	1979	1999	2019
Top-1% wealth share (%)				
Data (WID)	27.7	23.2	31.8	34.8
Model, channel on	27.6	29.0	32.1	34.8
Model, channel off	27.6	25.8	23.6	20.9
Common net return r (%)				
Model, channel on	2.01	1.77	1.37	0.86
Model, channel off	2.01	1.94	1.86	1.76
Wealth-weighted total return $\bar{r}_W$ (%)				
Model, channel on	3.41	3.35	3.29	3.23
Model, channel off	3.41	3.33	3.23	3.11

Note: Channel on uses the ICT-linked rule ($\psi = \psi^\star$); channel off retains persistent return differences at their 1967 dispersion ($\psi = 0$). Total return $\bar{r}_W$ is wealth-weighted, net of depreciation, and before the financing tax. After financing, aggregate capital income is rA. Wealth shares are window means; returns use the reported allocation and its evaluated stationary distribution.

[21] Hubmer, Krusell, and Smith (2021) also find that increased earnings risk lowers top wealth shares in their transition experiments.

Table A.10: The decline under fixed return dispersion: a partial-equilibrium decomposition

Values applied	Top-1% share (%)	Change from 1967 (pp)
1967 equilibrium	27.64	–
2019 wages and education cost	25.34	−2.30
2019 common return and lump-sum tax	22.52	−5.12
Both sets of 2019 values	20.86	−6.78

Note: Each experiment starts from the 1967 equilibrium and replaces the indicated values with those of the 2019 fixed-dispersion equilibrium. Household choices and the stationary distribution respond at the specified prices, tax, and education cost. The two middle rows each change one set of values; the final row changes both. Their interaction is +0.64 percentage points. Statistics are evaluated at the reported allocations; differences use unrounded values.

Table A.11: Tail shape and the return gradient

	Slope, top 1–0.1%	Slope, top 5–1%	Return, top 1% − median (pp)
1967	1.35	1.66	+2.34
Channel on, 1979	1.29	1.61	+2.52
Channel off, 1979	1.38	1.70	+2.32
Channel on, 1999	1.20	1.52	+2.86
Channel off, 1999	1.42	1.75	+2.33
Channel on, 2019	1.11	1.40	+3.32
Channel off, 2019	1.47	1.82	+2.43

Note: Local Hill-type slopes describe the stated population bands of the evaluated stationary wealth distribution.

Table A.12: Top-1% wealth shares at selected years

Year	Model, channel on	Model, channel off	WID top 1%
1967	27.6	27.6	27.7
1989	30.2	25.0	—
2016	34.8	21.4	—
2019	34.8	20.9	34.8

Note: All years use the baseline calibration. Channel on uses the ICT-linked rule ($\psi = \psi^{\star}$); channel off retains initial dispersion ($\psi = 0$). The 1989 and 2016 shares are additional model outcomes. Model shares are window means; reported changes use unrounded values. Dashes mark years for which WID values are not reported in this table.

D.4 Return dispersion, persistence, and schooling

Figure A.1 shows the calibration of ψ and the 2019 common return as dispersion widens. Tables A.13, A.14, and A.15 report the dispersion sweep, counterfactual comparisons, and persistence experiments. Table A.16 gives the schooling and affordability outcomes behind Table 6.

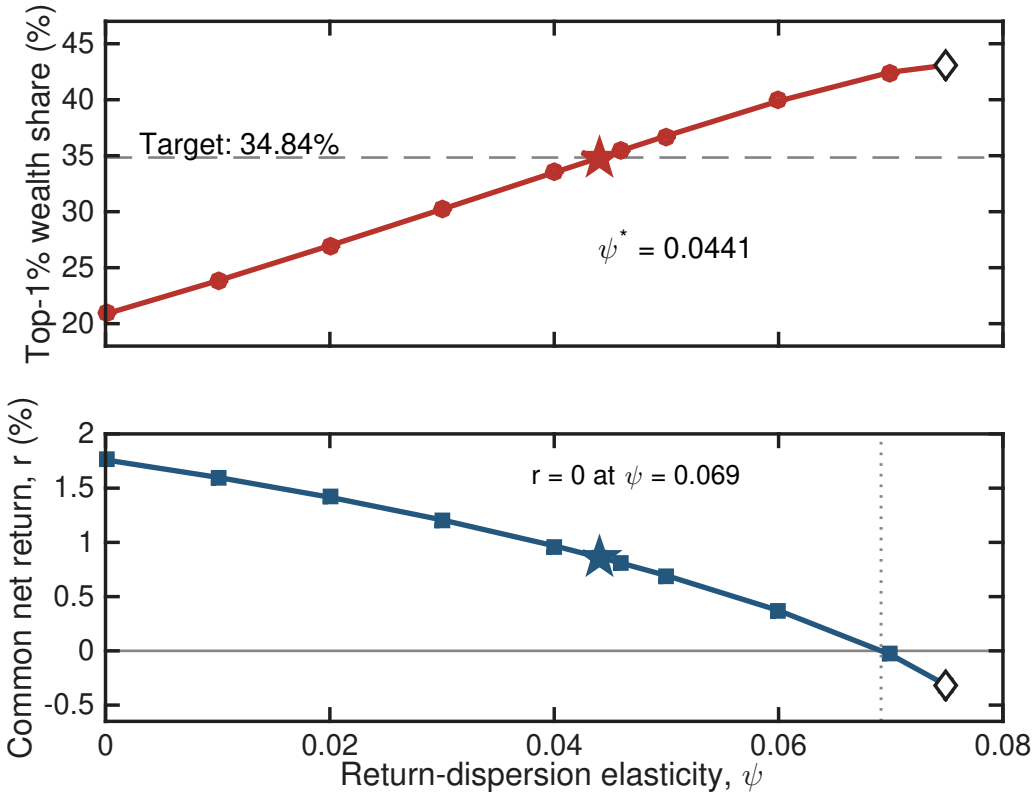


Figure A.1: Calibration of the return-dispersion channel

Note: The panels show the 2019 top-1% share (top) and common net return r (bottom) as the ICT-linked elasticity ψ varies, holding other inputs fixed. At $\psi = 0$, persistent return differences retain their 1967 dispersion. The star marks $\psi^\star$; the dashed line is the initial model top share plus the observed 1967–2019 increase. The dotted line marks the interpolated zero of r near $\psi = 0.069$; the diamond marks the last computed equilibrium, at $\psi = 0.075$.

Table A.13: Return dispersion and wealth concentration in 2019

ψ	Return SD (pp)	r (bp)	Top 1%	Local slope highest-return type	Top 1% $\bar{a}$ = 4,000	Financing margin
0.0000	6.00	176	20.86	1.102	21.70	0.105
0.0100	6.41	160	23.83	1.037	25.01	0.100
0.0200	6.85	142	26.97	0.976	28.52	0.094
0.0300	7.32	121	30.22	0.921	32.14	0.087
0.0400	7.84	97	33.50	0.868	35.81	0.078
0.0441*	8.06	86	34.84	0.848	37.31	0.074
0.0458	8.15	81	35.41	0.839	—[a]	0.072
0.0500	8.39	69	36.77	0.819	39.43	0.067
0.0600	8.99	37	39.88	0.772	42.85	0.053
0.0700†	9.67	-4	42.46	0.728	45.65	0.031
0.0750†	10.05	-32	43.09	0.706	45.78	0.014

Note: The baseline grid has 300 nodes and bound 2,000. Top shares are window means; r is the common net return in basis points. The local slope is minus the fitted slope of $\log \Pr(\text{wealth} \geq a)$ on $\log a$ for the highest-return type over $[\bar{a}/16, \bar{a}/4)$. The $\psi = 0.0458$ row uses the slope-targeted calibration's elasticity with all other parameters at baseline values. *Calibrated baseline elasticity. †Negative common return.
The financing margin $w_m z_\ell - \tau$ is the lowest labor income minus the financing tax, in model units; it must be positive for consumption at zero wealth. The common return crosses zero near $\psi = 0.069$. The baseline parameter sweep reaches $\psi = 0.075$.
[a]Wider-bound result unavailable at this elasticity.

Table A.14: Counterfactual 2019 wealth shares with fixed and wider return dispersion

Experiment	Channel on	Channel off	Difference (pp)	Relative to baseline
Baseline	34.8	20.9	+13.98	1.00
Proportional financing[a]	32.5	19.6	+12.90	0.92
Task-neutral technology[b]	39.1	25.0	+14.17	1.01
1967 ICT depreciation[b]	34.8	20.9	+13.90	0.99
1967 depreciation and tuition[b]	33.7	19.8	+13.82	0.99

Note: Each cell is a 2019 equilibrium on the baseline grid; shares are window means. The final column is the on-minus-off effect divided by its baseline value.
[a]A proportional levy finances return premia in place of the lump-sum tax. Baseline and levy rows use the ICT-linked rule: $\psi = \psi^\star$ on and $\psi = 0$ off.
[b]These rows fix premia at F_{19} on and F_{67} off.

Table A.15: Return persistence and wealth concentration in 2019

Expected spell (years)	Top 1%, on	r (%), on	Difference (pp)	Top 1%, off	r (%), off
7.28	—[a]	—	—	35.4	0.88
6.23	43.5	-0.09	+13.25	30.2	1.23
5.13	38.1	0.58	+14.23	23.9	1.60
4.64*	34.8	0.86	+13.98	20.9	1.76
3.96	29.5	1.26	+12.91	16.5	1.99
2.72	17.7	1.98	+8.21	9.5	2.37
2.07	11.6	2.33	+4.64	6.9	2.55
1.40	6.8	2.66	+1.73	5.1	2.72

Note: On fixes premia at F_{19}; off fixes them at F_{67}. Expected duration is $[p_{\text{die}} + (1 - p_{\text{die}})p_{\text{ref}}]^{-1}$, including refresh and death. Only the refresh probability varies. *Baseline duration. Shares are window means; r is the common net return.
[a]The wider-dispersion solution is unavailable at this duration; Appendix C reports the financing constraint.

Table A.16: Education and the return channel in 2019: two restrictions on college entry

Channel	Education	College	Top 1%	Top 10%	Gini	Below the 2019 tuition[a] Households	Newborns
Panel A: the 2019 economies							
On	Endogenous	29.8	34.8	60.8	0.720	67.5	67.1
On	1967 entry rule fixed	26.5	34.7	60.6	0.720	67.9	67.5
On	1967 college share fixed	13.1	34.9	60.8	0.723	71.6	71.4
Off	Endogenous	32.6	20.9	48.5	0.630	63.9	63.5
Off	1967 entry rule fixed	29.4	20.7	48.3	0.629	64.2	63.8
Off	1967 college share fixed	13.1	20.4	48.1	0.631	68.3	68.1

Panel B: top-1% effects (points)	Entry rule fixed	College share fixed
Return channel, education endogenous	+13.98	+13.98
Return channel, entry restricted	+14.05	+14.47
Restriction, channel on	−0.12	+0.03
Restriction, channel off	−0.19	−0.47
Interaction	+0.07	+0.50

Panel C: on − off (points)	Endogenous	Entry rule fixed	College share fixed
College share	−2.77	−2.96	0.00
Households below tuition	+3.63	+3.72	+3.34
Newborns below tuition	+3.68	+3.77	+3.34

Note: On uses the ICT-linked rule ($\psi = \psi^\star$); off retains initial dispersion ($\psi = 0$). Shares are percentages; top shares and the Gini are window means, and college is evaluated at the reported allocation. Fixing the 1967 entry rule applies its probabilities to 2019 newborns; fixing the 1967 college share rescales each economy's entry probabilities to keep that share at 13.10%. Both retain 2019 tuition and its affordability constraint. Entry restrictions affect the population transition; households continue to value the endogenous schooling option for descendants. Restriction effects are restricted minus endogenous top shares; the interaction is the on-minus-off difference in these effects. A positive interaction means endogenous schooling dampens the channel.
[a]Share with inherited assets (newborns) or current assets (households) below tuition, using within-cell weights consistent with the college-entry rule.

D.5 Additional robustness results

Figure A.2 and Table A.17 compare discount factors. Tables A.18 and A.19 report the numerical grid and tail checks. Table A.20 adds a change-of-units check and a local productivity experiment to the measured-productivity comparison in the main text. The units check scales wealth, wages, and output while leaving shares and return rates unchanged to numerical precision. The local experiment raises productivity by 5%, with the asset bound and taste scale fixed; its distributional effects therefore also reflect the change in their scale relative to the economy. Table A.21 reports alternative wealth targets and the corresponding dispersion elasticities.

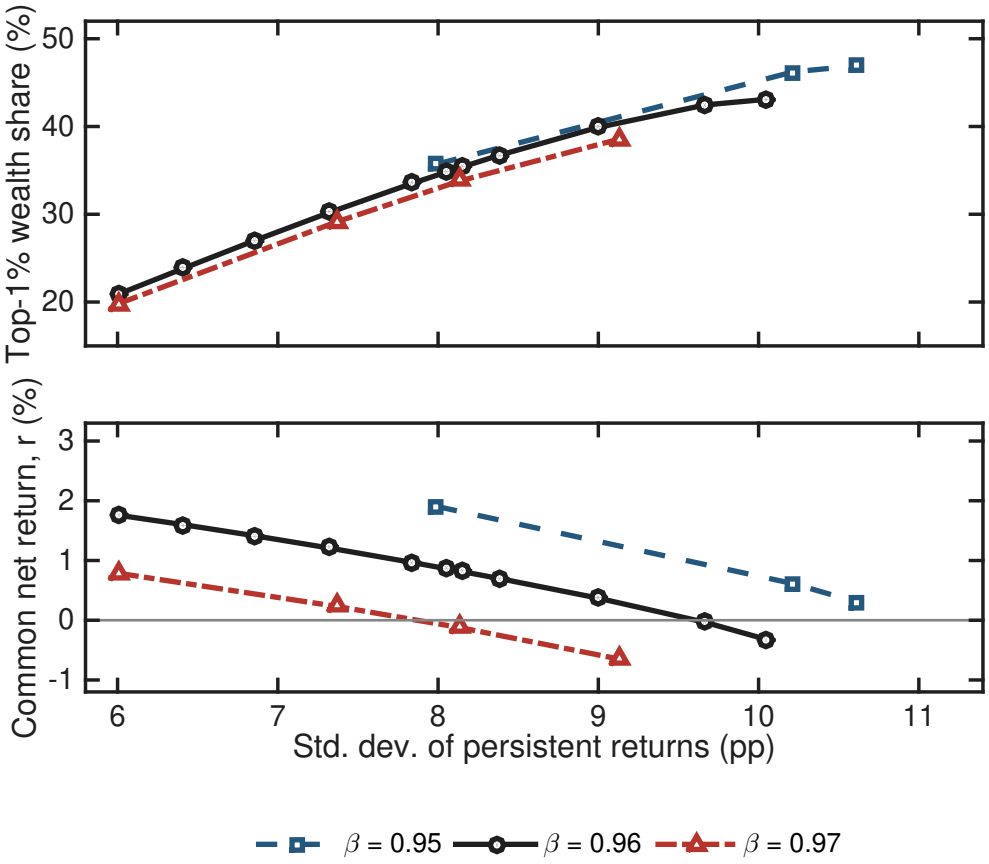


Figure A.2: Return dispersion and the discount factor

Note: The panels show the 2019 top-1% share (top) and common net return (bottom) against the standard deviation of persistent return premia at three discount factors. Each point is a stationary equilibrium at the 2019 inputs on the baseline asset grid, with all remaining parameters held fixed. Table A.17 reports the numerical values.

Table A.17: Sensitivity to the discount factor, 2019

β	ψ	Return SD (pp)	r (%)	Top 1%
0.95	0.0441	7.99	1.91	35.69
0.95	0.0800	10.22	0.61	46.22
0.95	0.0850	10.61	0.31	46.92
0.96	0.0000	6.00	1.76	20.86
0.96	0.0100	6.41	1.60	23.83
0.96	0.0200	6.85	1.42	26.97
0.96	0.0300	7.32	1.21	30.22
0.96	0.0400	7.84	0.97	33.50
0.96	0.0441	8.06	0.86	34.84
0.96	0.0458	8.15	0.81	35.41
0.96	0.0500	8.39	0.69	36.77
0.96	0.0600	8.99	0.37	39.88
0.96	0.0700	9.67	-0.04†	42.46
0.96	0.0750	10.05	-0.32†	43.09
0.97	0.0000	6.00	0.79	19.77
0.97	0.0300	7.37	0.23	29.17
0.97	0.0441	8.14	-0.12†	33.81
0.97	0.0600	9.13	-0.65†	38.56

Note: Each economy uses the baseline asset grid and holds all parameters other than β and ψ at their baseline values. The table reports solved elasticity values for each discount factor. The $\psi = 0.0458$ row uses the slope-targeted calibration's elasticity with the remaining parameters at baseline values. †Negative common return.

Table A.18: Sensitivity to the asset grid, 2019

Grid $(n_a, \bar{a})$	ψ	Top 1%	r (%)	
(300, 2,000)	0.0441	34.84	+0.860	baseline
(600, 2,000)	0.0441	34.85	+0.866	finer, same bound
(300, 4,000)	0.0441	37.31	+0.793	wider bound, same nodes
(600, 4,000)	0.0441	37.31	+0.798	finer and wider
(300, 8,000)	0.0441	39.46	+0.728	wider bound
(300, 16,000)	0.0441	41.35	+0.666	wider bound
(600, 2,000)	0	20.78	+1.765	finer, channel off

Note: Each row solves the equilibrium on the indicated grid, holding calibrated parameters fixed. Wider dispersion uses $\psi = \psi^{\star}$; the final row uses fixed dispersion ($\psi = 0$). Shares are window means; r is the common net return.

Table A.19: Wealth-tail slopes and approximate tail exponents

Bound $\bar{a}$	Local slope highest-return type	Local slope all households	Single-type exponent	Mixture exponent
1967				
2,000	1.072	1.165	1.136	1.126
4,000	1.070	1.142	1.132	1.096
8,000	1.068	1.130	1.129	1.063
16,000	1.066	1.125	1.127	1.041
2,000, 13 return nodes	0.883	1.166	0.900	0.900
2019, fixed dispersion				
2,000	1.102	1.280	1.148	1.146
4,000	1.100	1.242	1.142	1.139
8,000	1.097	1.218	1.137	1.133
16,000	1.096	1.205	1.134	1.127
2,000, 13 return nodes	0.894	1.279	0.907	0.907
2019, $\psi^\star$				
2,000	0.848	1.070	0.886	0.886
4,000	0.847	1.041	0.881	0.880
8,000	0.847	1.022	0.876	0.875
16,000	0.846	1.011	0.873	0.871
2,000, 13 return nodes	0.692	1.067	0.705	0.705

Note: Local slopes are minus the fitted slopes of the log share with wealth at least a on $\log a$, using asset points in $[\bar{a}/16, \bar{a}/4)$. Smaller slopes indicate thicker tails. The single-type exponent uses the fastest-growing return type and its persistence; the mixture exponent also accounts for switches among return types. Both approximate the rate of wealth growth within each type as constant. The single-type exponent is an upper bound on the mixture exponent under this approximation. An exponent at or below one implies an infinite mean under the constant-growth approximation. The 1967 mixture estimates at bounds 4,000–16,000 are sensitive to small changes in the approximated growth rates. These are diagnostics for the bounded model. Nine return-type points are used unless marked.

Table A.20: Neutral productivity: 2019 equilibria at measured and local productivity levels

Economy	Top 1%	r (%)	College (%)	A	K_c	Channel effect (pp)
A. Baseline, 2019 ($Z = 1$)						
Channel off ($\psi = 0$)	20.9	1.76	32.6	2.473	0.255	
Channel on ($\psi^\star$)	34.8	0.86	29.8	2.949	0.276	+13.98
B. Measured 2019 productivity, $Z = 2.128$ ($s = 2.80$)						
ICT-linked dispersion, channel off	19.6	1.72	39.2	7.877	0.796	
ICT-linked dispersion, channel on	33.6	0.81	35.3	9.373	0.858	+14.01
Premia fixed at F_{67}[a], channel off	19.6	1.72	39.2	7.877	0.796	
Premia fixed at F_{19}[a], channel on	33.4	0.83	35.3	9.334	0.857	+13.79
C. Units check[b], $Z = 2.128$						
Channel on, all units scaled	34.8	0.86	29.8	8.256	0.276	
Difference from the 2019 baseline	$+2.3 \times 10^{-6}$	-1.4×10^{-7}	-4.9×10^{-7}	-4.6×10^{-8} [c]		
D. Local productivity change[d], $Z = 1.05$						
Premia fixed at F_{19}, $Z = 1$	34.8	0.86	29.8	2.949	0.276	
Premia fixed at F_{19}, $Z = 1.05$	34.6	0.87	29.9	3.149	0.276	
Difference	−0.24	+0.007	+0.12	+6.8%	+0.00%	

Note: All economies use 300 asset nodes. Z is neutral productivity relative to 1967 and $s = Z^{1/(1-\alpha)}$. Panel B scales tuition, the asset grid, and K_c^{ref} by s, and the taste scale by $s^{-0.5}$, keeping the ICT price at its measured value. Wealth A is in each row's model units. Top shares are window means; channel effects are on minus off within each pair. ICT-linked rows use $\psi = \psi^\star$ on and $\psi = 0$ off.
[a] Premia fixed at F_{19} on and F_{67} off.
[b] Units check: tuition, ICT price, and asset grid scale by s, and the taste scale by $s^{-0.5}$, with F_{19} fixed. Wealth, wages, and output scale by s; physical ICT capital, shares, and returns are invariant. Differences in percentage points.
[c] $A/(sA_{2019}) - 1$.
[d] $Z = 1.05$, with tuition and ICT price scaled by s and the asset grid and taste scale held fixed; premia remain at F_{19}. The comparator is the same economy at $Z = 1$. Differences are in percentage points, except A and K_c (percent).

Table A.21: Alternative wealth targets and return distributions

Specification	ψ	2019 return SD (pp)	Top 1%	Top 10%	Middle 60%	r (%)
Baseline (Normal)	0.0441	8.1	34.8	60.8	25.8	0.86
SZZ target (Normal)	0.0553[a]	—	38.4	—	—	0.52
CBO target (Normal)	0.0587	—	39.5	—	—	0.41
Mixture: 1967 recalibrated	0.060	—	43.7	—	—	0.46
Mixture: initial share matched	0.0441	—	29.9	—	—	1.77

Note: WID is the World Inequality Database; SZZ denotes Smith, Zidar, and Zwick (2023); CBO denotes the Congressional Budget Office (2022). The alternative targets are increases of 6.6 percentage points over 1989–2016 (SZZ) and 7.4 points over 1989–2019 (CBO). Wealth shares are percentages of total wealth.
All values are for 2019. The alternative-series rows interpolate between the solved $\psi = 0.050$ and 0.060 equilibria at the elasticity that matches each series' window. The mixture rows use the specifications in Panels A and B of Table 8, respectively. A dash denotes an unreported statistic.
[a] The SZZ matching elasticity is extrapolated by 0.0003 beyond the largest solved value for the 1989–2016 window, $\psi = 0.055$.